Second-order number-conserving description of nonequilibrium dynamics in finite-temperature Bose-Einstein condensates

T. P. Billam*
Jack Dodd Centre for Quantum Technology, Department of Physics, University of Otago, Dunedin 9016, New Zealand

P. Mason and S. A. Gardiner
Joint Quantum Centre (JQC) Durham-Newcastle, Department of Physics, Durham University, Durham, DH1 3LE, United Kingdom
(Received 11 July 2012; revised manuscript received 6 March 2013; published 27 March 2013)

While the Gross-Pitaevskii equation is well established as the canonical dynamical description of atomic Bose-Einstein condensates (BECs) at zero temperature, describing the dynamics of BECs at finite temperatures remains a difficult theoretical problem, particularly when considering low-temperature, nonequilibrium systems in which depletion of the condensate occurs dynamically as a result of external driving. In this paper, we describe a fully time-dependent numerical implementation of a second-order, number-conserving description of finite-temperature BEC dynamics. This description consists of equations of motion describing the coupled dynamics of the condensate and noncondensate fractions in a self-consistent manner, and is ideally suited for the study of low-temperature, nonequilibrium, driven systems. The δ-kicked-rotor BEC provides a prototypical example of such a system, and we demonstrate the efficacy of our numerical implementation by investigating its dynamics at finite temperature. We demonstrate that the qualitative features of the system dynamics at zero temperature are generally preserved at finite temperatures, and predict a quantitative finite-temperature shift of resonance frequencies which would be relevant for, and could be verified by, future experiments.

DOI: 10.1103/PhysRevA.87.033628 PACS number(s): 03.75.Kk, 67.85.De, 05.30.Jp

I. INTRODUCTION

Even at zero temperature, typical atomic Bose-Einstein condensates (BECs) contain a small noncondensate fraction due to interatomic interactions. In real experiments, which necessarily take place at finite temperatures and may involve dynamical depletion of the condensate [1]—for instance, due to nonequilibrium dynamics induced by changes in applied external fields, a non-negligible noncondensate fraction often arises. A full understanding of the dynamics of such systems requires a fully dynamical, finite-temperature theoretical description which goes beyond the mean-field, zero-temperature Gross-Pitaevskii equation (GPE). Due to the complexity of such descriptions, the nonequilibrium dynamics of atomic BECs in the presence of a significant noncondensate fraction (whether thermal or dynamical in origin) remains a largely open problem [2,3].

In systems where the noncondensate fraction is primarily thermal in origin, a variety of theoretical descriptions have been developed and successfully applied to nonequilibrium atomic BEC dynamics. These include *symmetry-breaking* descriptions, which are based on a perturbative expansion about a mean field; for example, the Hartree-Fock-Bogoliubov-Popov (HFBP) description [4–7], and the Zaremba-Nikuni-Griffin (ZNG) description [8–14]. Other successful descriptions have been obtained in the context of *c-field* methods, reviewed in Ref. [15], which describe the highly occupied modes of the system as a classical field. These descriptions include the projected Gross-Pitaevskii equation (PGPE) [16–18], the stochastic projected GPE (SPGPE) [19,20] and stochastic GPE (SGPE) [2,21–26], and the truncated Wigner PGPE [27–30].

However, the nonequilibrium dynamics of systems in which a low-temperature BEC is driven by an applied external field leading to *dynamical* depletion of the condensate have not been as widely investigated. The prime example of such systems are atomic BEC analogs of generic quantum chaotic systems; e.g., the kicked accelerator [31,32], kicked harmonic oscillator [33–35], and kicked rotor [36–41]. These systems offer an excellent test bed for exploring generic issues of quantum chaos [38,42], quantum superposition [43], quantum resonances [33,39,40], dynamical instability and dynamical depletion [35,36,39,40], and even entropy, thermalization, and integrability [44–46]. A particular issue in the description of these systems is the occurrence of nonlinear quantum resonances [40]: values of the system parameters at which the system resonantly absorbs energy from the driving. Such resonances are an extremely generic feature of these systems, and are sensitive to the value of the nonlinearity (product of s-wave scattering length a_s and condensate occupation N_c). Consequently, one expects the dynamical depletion of the condensate caused by the driving to rapidly and fundamentally alter the subsequent dynamics of the system close to these resonances, compared to the predictions of the Gross-Pitaevskii equation [1].

The rapid and severe back-action of condensate depletion on the nonequilibrium dynamics of these systems presents considerable challenges for the above-mentioned finite-temperature descriptions. In particular, the PGPE and SPGPE are fundamentally restricted to a high-temperature regime, and lack a quantum treatment of the pair-excitation processes which drive condensate depletion. In principle the truncated-Wigner PGPE may be used to model nonequilibrium dynamics of driven systems at low (and zero) temperatures [47]. However, in order to go beyond a close-to-equilibrium approximation in which the condensate remains in its initial

*thomas.billam@otago.ac.nz

state, one must obtain the dynamics of the condensate within such a treatment from an ensemble average of individual GPE trajectories. While such a treatment is entirely possible, and can, for example, be conducted by determining the single-particle density matrix in a number-conserving fashion [48], the issues of spurious thermalization and inaccurate long-time dynamics in the truncated Wigner method (see, e.g., Refs. [15,49]) would necessitate a very careful approach when applying such a treatment to the nonequilibrium dynamics of driven systems.

In order to comprehensively describe such systems one must thus self-consistently capture the back-action of the increasing population of, and the subsequent dynamics in, low-lying noncondensate excitations on the condensate. To achieve this, a description which consistently divides the system into well-defined condensate and noncondensate fractions at all times would appear to be necessary (as opposed to a c-field description in which the condensate fraction must be extracted by subsequent ensemble averaging). In that they comprise a set of coupled equations for the condensate and the noncondensate components, symmetry-breaking descriptions would thus appear to offer a more appropriate treatment of low-temperature driven systems. However, all such dynamical descriptions which have been applied to BEC dynamics to date have contained an approximate treatment of pair-excitation processes that neglects the anomalous average; while suitable at higher temperatures, this leads to descriptions which incompletely model the phonon character of elementary excitations at low temperatures [50]. Furthermore, the assumption of a symmetry-broken condensate state, and hence overall number nonconservation, in any symmetry-breaking method presents an additional potential problem; since the prime contribution to the departure from GPE dynamics in low-temperature driven systems results from, and can be extremely sensitive to, changes in the number of condensate particles, conservation of the total atom number appears to be necessary in order to obtain a fully self-consistent description of such systems as realized in atomic BEC experiments (in which the total atom number is finite and fixed) [51]. In a formal sense, coupled equations of motion for the condensate and noncondensate within a symmetry-breaking treatment do not contain any terms to explicitly preserve the orthogonality of the condensate and noncondensate modes (see Sec. II A); in the context of low-temperature driven systems, this means an ambiguity in interpreting the solutions of those equations for anything other than short times.

In view of the above considerations number-conserving descriptions [52–56], in which the system is partitioned into manifestly orthogonal condensate and noncondensate parts using the Penrose-Onsager criterion [57], are, in principle, ideally suited to this regime. However, until recently only the first-order number-conserving description of Gardiner [53] and Castin and Dum [52] offered a description which was numerically tractable in fully time-dependent form. Application of this first-order number-conserving description to the δ-kicked-rotor BEC [36,37,39] and δ-kicked-harmonic-oscillator BEC [35,58] revealed a general tendency for rapid, unbounded growth. Unfortunately, as the equation describing the condensate in this first-order treatment is simply the GPE, this rapid, unbounded growth can be viewed as a consequence of linearized instabilities present in the GPE, which would be removed by a higher-order description containing a self-consistent back-action of the noncondensate on the condensate [1]. Thus, similar to the methods discussed above, the first-order description is also of limited use in describing the long-time dynamics of low-temperature, driven BEC systems.

However, such a self-consistent back-action *is* present within a second-order number-conserving description, such as presented by Gardiner and Morgan in Ref. [51] and previously used highly successfully by Morgan [59–61] to calculate, using a linear response treatment, the excitation frequencies of a BEC at finite temperature as measured in experiments at JILA [62,63] and MIT [64,65]. Recently [41], the first fully time-dependent implementation of the second-order number-conserving equations of motion was applied to an initially zero-temperature δ-kicked-rotor BEC. This application revealed that the second-order description's self-consistent back-action does indeed damp out the unbounded growth in noncondensate fraction seen in the first-order description. Consequently, the time-dependent form of the second-order number-conserving description provides an excellent tool for studying the nonequilibrium dynamics of driven BECs at low temperatures.

The purpose of this paper is primarily to present, in detail, analytic and numerical techniques which allow one to evolve the second-order number-conserving equations of motion at finite temperatures, enabling a systematic exploration of nonequilibrium BEC dynamics at finite temperatures. A restricted subset of these techniques, limited to zero-temperature initial conditions, were used to obtain the results in Ref. [41], but were not described in detail in that work. We also use these techniques to conduct a finite-temperature study of the nonequilibrium dynamics of the δ-kicked-rotor BEC, extending the results of Ref. [41] and previous works. Remarkably, we observe that many of the sharp nonlinear resonance features observed at zero temperature in Refs. [40,41] are qualitatively preserved at temperatures sufficient to cause significant initial condensate depletion. In particular, our exploration of the effects of initial temperature predicts a finite-temperature shift in the system's resonance frequencies which could be experimentally measured and verified.

The remainder of the manuscript is structured as follows: We begin by introducing, in Sec. II, the second-order number-conserving description of the dynamics and present the second-order equations of motion in their most general form. We give a detailed discussion of the self-consistent properties and regime of validity of the resulting description at both zero and finite temperatures. In particular, we discuss potential problems finding equilibrium initial conditions at higher temperatures. In Sec. III we develop a numerical method to evolve initial states according to the second-order equations of motion. This method explicitly includes the nonlinear, nonlocal terms coupling the condensate and the quasiparticle modes. It is these terms which maintain orthogonality between the condensate and noncondensate, and which are particularly difficult to deal with in the context of general numerical integration schemes. In Sec. IV we apply the method to systematically explore the effects of finite initial temperatures in the δ-kicked-rotor BEC. We also extend the analysis of this system given in Ref. [41] by further exploring the contrast between first-

and second-order descriptions, and analyzing the evolution of the single-particle von Neumann entropy. We predict a shift of resonance frequencies at finite temperature which could feasibly be detected in experiments. Section V comprises the conclusions. A technical Appendix follows, in which we present details of our numerical technique.

II. SECOND-ORDER, NUMBER-CONSERVING THEORETICAL DESCRIPTION

A. Motivation

We consider a system of N bosonic atoms of mass m, confined by an external potential $V(\mathbf{r},t)$, and interacting via pairwise s-wave contact interactions. The Hamiltonian for such a system is given by

$$\hat{H} = \int d\mathbf{r}\, \hat{\Psi}^\dagger(\mathbf{r}) \left[H_{\rm sp}(\mathbf{r},t) + \frac{U_0}{2}\hat{\Psi}^\dagger(\mathbf{r})\hat{\Psi}(\mathbf{r}) \right] \hat{\Psi}(\mathbf{r}), \quad (1)$$

where $\hat{\Psi}(\mathbf{r})$ and $\hat{\Psi}^\dagger(\mathbf{r})$ are second-quantized field operators obeying standard equal-time bosonic commutation relations. Here, the single-particle Hamiltonian is

$$H_{\rm sp}(\mathbf{r},t) = -\frac{\hbar^2}{2m}\nabla^2 + V(\mathbf{r},t), \quad (2)$$

where

$$U_0 = \frac{4\pi\hbar^2 a_s}{m}, \quad (3)$$

for s-wave scattering length a_s.

Computing the full many-body dynamics of such a system directly from the Hamiltonian Eq. (1) is, in general, an intractable problem. However, in the case where N is large and the majority of the system is Bose-Einstein condensed, one can obtain an approximation to the full many-body dynamics via a perturbative description, in which the noncondensate fraction constitutes the small parameter. To develop such a description, we adopt the definition of Bose-Einstein condensation—applicable to a finite-size and interacting system as described by Eq. (1)—given by Penrose and Onsager [57]. In this definition the condensate mode, $\phi_c(\mathbf{r},t)$, is identified as a single macroscopically occupied eigenstate of the single-particle density matrix,[1]

$$\rho(\mathbf{r},\mathbf{r}',t) = \langle \hat{\Psi}^\dagger(\mathbf{r}')\hat{\Psi}(\mathbf{r})\rangle. \quad (4)$$

Consequently, the condensate mode $\phi_c(\mathbf{r},t)$ satisfies

$$\int d\mathbf{r}' \rho(\mathbf{r},\mathbf{r}',t)\phi_c(\mathbf{r}',t) = N_c(t)\phi_c(\mathbf{r},t), \quad (5)$$

where the condensate mode occupation $N_c(t)$ is taken to be much greater than all other single-particle mode occupations [given by the other eigenvalues of $\rho(\mathbf{r},\mathbf{r}',t)$] at any time.

Using this definition, one can explicitly partition the field operator into a condensate part, $\hat{a}_c(t)\phi_c(\mathbf{r},t)$, and a noncondensate part, $\delta\hat{\Psi}(\mathbf{r},t)$:

$$\hat{\Psi}(\mathbf{r}) = \hat{a}_c(t)\phi_c(\mathbf{r},t) + \delta\hat{\Psi}(\mathbf{r},t). \quad (6)$$

[1]Note that in Eq. (4) the brackets $\langle\cdots\rangle$ denote an expectation value with respect to the full many-particle density matrix; at finite temperature this involves a thermal, as well as a quantum, average.

Here, the condensate annihilation operator $\hat{a}_c(t)$ annihilates an atom in the condensate mode $\phi_c(\mathbf{r},t)$. To maintain Hermiticity of the single-particle density matrix one must ensure that the part of the field operator describing the condensate mode, $\hat{a}_c(t)\phi_c(\mathbf{r},t)$, is explicitly orthogonal to the part describing the noncondensate, $\delta\hat{\Psi}(\mathbf{r},t)$, at all times. Formally, one defines

$$\delta\hat{\Psi}(\mathbf{r},t) = \int d\mathbf{r}'\, \mathcal{Q}(\mathbf{r},\mathbf{r}')\hat{\Psi}(\mathbf{r}',t), \quad (7)$$

where

$$\mathcal{Q}(\mathbf{r},\mathbf{r}') = \delta(\mathbf{r}'-\mathbf{r}) - \phi_c(\mathbf{r})\phi_c^*(\mathbf{r}'), \quad (8)$$

and hence one sees that $\phi_c(\mathbf{r},t)$ and $\delta\hat{\Psi}(\mathbf{r},t)$ are "orthogonal" in the sense that

$$\int d\mathbf{r}\phi_c^*(\mathbf{r},t)\delta\hat{\Psi}(\mathbf{r},t) = 0. \quad (9)$$

This partition is *number conserving*, in the sense that the system remains in a state of fixed total atom number.

This *number-conserving* partition can be contrasted with the *symmetry-breaking* partition used in other finite temperature descriptions, which is based on a partition of the field operator into a finite expectation value (or order parameter), $\Psi(\mathbf{r},t) = \langle\hat{\Psi}(\mathbf{r})\rangle$, and an operator-valued fluctuation $\hat{\delta}(\mathbf{r},t)$,

$$\hat{\Psi}(\mathbf{r}) = \Psi(\mathbf{r},t) + \hat{\delta}(\mathbf{r},t). \quad (10)$$

Two related consequences of the symmetry-breaking partition [Eq. (10)] are a breaking of the overall $U(1)$ phase symmetry of the Hamiltonian, and a general lack of orthogonality between the condensate and noncondensate parts of the system. Specifically, having constructed a perturbative description in terms of $\Psi(\mathbf{r},t)$ and $\hat{\delta}(\mathbf{r},t)$ one generically finds that, in the case of an inhomogeneous order parameter, $\Psi(\mathbf{r},t)$ and $\hat{\delta}(\mathbf{r},t)$ are not orthogonal in the sense of Eq. (9). As a result, one cannot uniquely reassemble a Hermitian density matrix for the system from $\Psi(\mathbf{r},t)$ and $\hat{\delta}(\mathbf{r},t)$, as one can from $\phi_c(\mathbf{r},t)$ and $\delta\hat{\Psi}(\mathbf{r},t)$. This lack of an explicit, time-independent orthogonality between condensate and noncondensate [in the sense of Eq. (9)] also means that one cannot unambiguously determine the condensate population N_c, and the noncondensate population N_t, associated with the symmetry-breaking partition. In the context of driven low-temperature BECs, where the dynamics are extremely strongly influenced by changes in N_c, this ambiguity in the condensate population constitutes a genuine disadvantage of the symmetry-breaking approach.

A number-conserving description of the system's dynamics is obtained by treating the noncondensate part $\delta\hat{\Psi}(\mathbf{r},t)$ perturbatively, by means of an expansion in terms of a suitable fluctuation operator [51–53]. Neglecting the noncondensate completely yields a zeroth-order description in the form of the Gross-Pitaevskii equation (GPE); this takes the form [we explicitly denote the condensate mode in this zeroth-order description by $\phi_c^{(0)}(\mathbf{r},t)$ for clarity in later sections],

$$i\hbar\frac{\partial\phi_c^{(0)}(\mathbf{r},t)}{\partial t} = \left[H_{\rm sp}(\mathbf{r},t) + \tilde{U}\left|\phi_c^{(0)}(\mathbf{r},t)\right|^2 - \lambda_0^{(0)}(t)\right]\phi_c^{(0)}(\mathbf{r},t), \quad (11)$$

where $\tilde{U} = U_0 N_c$, and $\lambda_0^{(0)}(t)$ is given by

$$\lambda_0^{(0)}(t) = \int d\mathbf{r}\phi_c^{(0)*}(\mathbf{r},t) \times \left[H_{\rm sp}(\mathbf{r},t) + \tilde{U}\left|\phi_c^{(0)}(\mathbf{r},t)\right|^2 - i\hbar\frac{\partial}{\partial t}\right]\phi_c^{(0)}(\mathbf{r},t). \quad (12)$$

As in Refs. [41,51,53], $\lambda_0^{(0)}(t)$ is defined in such a way as to be generally time dependent. However, as $\lambda_0^{(0)}(t)$ is explicitly real, the dynamics resulting from its time evolution consist only of an irrelevant global phase. When considering, as we do in this paper, the evolution of a stationary, equilibrium initial condition subject to a time-dependent perturbation, it is most convenient to work with a *time-independent* GPE eigenvalue $\lambda_0^{(0)}$ given by

$$\lambda_0^{(0)} = \int d\mathbf{r}\phi_c^{(0)*}(\mathbf{r},0)\left[H_{\rm sp}(\mathbf{r},0) + \tilde{U}\left|\phi_c^{(0)}(\mathbf{r},0)\right|^2\right]\phi_c^{(0)}(\mathbf{r},0), \quad (13)$$

where $\phi_c^{(0)}(\mathbf{r},0)$ represents the $t = 0$ stationary, equilibrium state of the GPE. Since several subtly different eigenvalues λ appear in the subsequent development, here we have introduced the convention that the *subscript* index to λ denotes the order (with respect to the noncondensate fluctuation operators) of the *functional* defining λ, while the bracketed *superscript* index to λ denotes the order of approximation of the condensate *wave function* appearing inside the functional definition. Furthermore, if any eigenvalue is time dependent we *always* denote this explicitly with a (t) argument. In the case where a time argument is absent, the corresponding eigenvalue should be understood as having been evaluated for the appropriate equilibrium initial condition.

To work with the time-independent eigenvalue $\lambda_0^{(0)}$ in the GPE description, one simply makes the replacement $\lambda_0^{(0)}(t) \to \lambda_0^{(0)}$ in Eq. (11). Note that while $\lambda_0^{(0)}$ arises naturally as a nonlinear eigenvalue during the development of a zeroth-order number-conserving equation of motion, at this level of approximation it is equivalent to the chemical potential μ, which would be introduced as a Lagrange multiplier to determine the average particle number in a symmetry-breaking approach.

In contrast to the GPE, the second-order number-conserving description we use in this paper provides a description of both the condensate and the noncondensate, and consists of mutually coupled equations for both, which we outline in the following section.

B. Equations of motion

Conducting a self-consistent, second-order, number-conserving expansion—as detailed in Ref. [51]—leads to a number-conserving generalized GPE (GGPE) for the dynamics of the condensate mode $\phi_c(\mathbf{r},t)$:

$$i\hbar\frac{\partial\phi_c(\mathbf{r})}{\partial t} = \left[H_{\rm sp}(\mathbf{r}) - \lambda_2^{(2)}(t)\right]\phi_c(\mathbf{r}) + \tilde{U}\left[\left(1 - \frac{1}{N_c}\right)|\phi_c(\mathbf{r})|^2 + 2\frac{\tilde{n}(\mathbf{r},\mathbf{r})}{N_c}\right]\phi_c(\mathbf{r}) + \tilde{U}\phi_c^*(\mathbf{r})\frac{\tilde{m}(\mathbf{r},\mathbf{r})}{N_c} - \tilde{U}\int d\mathbf{r}'\,|\phi_c(\mathbf{r}')|^2 \times \left(\frac{\tilde{n}(\mathbf{r},\mathbf{r}')}{N_c}\phi_c(\mathbf{r}') + \phi_c^*(\mathbf{r}')\frac{\tilde{m}(\mathbf{r},\mathbf{r}')}{N_c}\right). \quad (14)$$

Here we have introduced the convention, adopted generally hereafter, of omitting explicit time dependences wherever this aids clarity. The dynamics of the noncondensate enter the GGPE [Eq. (14)] through the normal $[\tilde{n}(\mathbf{r},\mathbf{r}')]$ and anomalous $[\tilde{m}(\mathbf{r},\mathbf{r}')]$ averages. These are, respectively, defined by

$$\tilde{n}(\mathbf{r},\mathbf{r}') = \langle\tilde{\Lambda}^\dagger(\mathbf{r}')\tilde{\Lambda}(\mathbf{r})\rangle, \quad (15)$$

and

$$\tilde{m}(\mathbf{r},\mathbf{r}') = \langle\tilde{\Lambda}(\mathbf{r}')\tilde{\Lambda}(\mathbf{r})\rangle, \quad (16)$$

where

$$\tilde{\Lambda}(\mathbf{r}) = \frac{1}{\sqrt{N_c}}\hat{a}_c^\dagger\delta\hat{\Psi}(\mathbf{r}), \quad (17)$$

is the number-conserving fluctuation operator in which a perturbative expansion has been conducted. Note that the corresponding small parameter is $\sqrt{N_t(t)/N_c(t)}$, where $N_t(t) = N - N_c(t)$ is the occupation of the noncondensate. We have also introduced the *complex, time-dependent* "GGPE eigenvalue" $\lambda_2^{(2)}(t)$, which is given by

$$\lambda_2^{(2)}(t) = \tilde{U}\int d\mathbf{r}\,\phi_c^*(\mathbf{r})^2\frac{\tilde{m}(\mathbf{r},\mathbf{r})}{N_c} + \int d\mathbf{r}\,\phi_c^*(\mathbf{r})\left\{H_{\rm sp}(\mathbf{r}) + \tilde{U}\left[\left(1 - \frac{1}{N_c}\right)|\phi_c(\mathbf{r})|^2 + 2\frac{\tilde{n}(\mathbf{r},\mathbf{r})}{N_c}\right] - i\hbar\frac{\partial}{\partial t}\right\}\phi_c(\mathbf{r}). \quad (18)$$

It is essential to emphasize that this "eigenvalue" is in general time dependent, and that Eq. (18) should be taken to be evaluated using the values of $\phi_c(\mathbf{r})$, N_c, etc., at a particular time. As we demonstrate in the subsequent section, this time dependence of $\lambda_2^{(2)}(t)$ is crucial in order to obtain self-consistent number dynamics. However, as in the case of the GPE [Eqs. (11) and (13)] it is considerably more convenient to work with a *real, time-independent* eigenvalue, and in Sec. III we will reformulate the second-order equations of motion in order to consistently (up to second order) replace $\lambda_2^{(2)}(t)$ with such a quantity.

The GGPE must be coupled to a consistent set of equations of motion for the noncondensate; at second order these consist of the number-conserving modified Bogoliubov–de Gennes equations (MBdGE):

$$i\hbar\frac{\partial}{\partial t}\begin{pmatrix}\tilde{\Lambda}(\mathbf{r})\\ \tilde{\Lambda}^\dagger(\mathbf{r})\end{pmatrix} = \int d\mathbf{r}'\begin{pmatrix}\mathcal{L}(\mathbf{r},\mathbf{r}') & \mathcal{M}(\mathbf{r},\mathbf{r}')\\ -\mathcal{M}^*(\mathbf{r},\mathbf{r}') & -\mathcal{L}^*(\mathbf{r},\mathbf{r}')\end{pmatrix}\begin{pmatrix}\tilde{\Lambda}(\mathbf{r}')\\ \tilde{\Lambda}^\dagger(\mathbf{r}')\end{pmatrix}, \quad (19)$$

where

$$\mathcal{L}(\mathbf{r},\mathbf{r}') = \delta(\mathbf{r} - \mathbf{r}')\left[H_{\rm sp}(\mathbf{r}') + \tilde{U}|\phi_c(\mathbf{r}')|^2 - \lambda_0^{(2)}(t)\right] + \int d\mathbf{r}''\,\mathcal{Q}(\mathbf{r},\mathbf{r}'')\tilde{U}|\phi_c(\mathbf{r}'')|^2\mathcal{Q}(\mathbf{r}'',\mathbf{r}'), \quad (20)$$

and

$$\mathcal{M}(\mathbf{r},\mathbf{r}') = \int d\mathbf{r}''\mathcal{Q}(\mathbf{r},\mathbf{r}'')\tilde{U}\phi(\mathbf{r}'')^2\mathcal{Q}^*(\mathbf{r}'',\mathbf{r}'). \quad (21)$$

The modification in these equations—with respect to the ordinary BdG equations obtained in a symmetry-breaking description—is the appearance of the projector $\mathcal{Q}(\mathbf{r},\mathbf{r}')$ which explicitly enforces the orthogonality of the condensate and noncondensate, and of the time-dependent "GPE eigenvalue" $\lambda_0^{(2)}(t)$. This "GPE eigenvalue" is obtained by substituting the GGPE condensate mode $\phi_c(\mathbf{r},t)$ into the GPE [Eq. (11)] in place of the GPE condensate mode $\phi_c^{(0)}(\mathbf{r},t)$, and allowing the eigenvalue to be generically time dependent. That is,

$$\lambda_0^{(2)}(t) = \int d\mathbf{r}\phi_c^*(\mathbf{r},t) \times \left[H_{\rm sp}(\mathbf{r},t) + \tilde{U}|\phi_c(\mathbf{r},t)|^2 - i\hbar\frac{\partial}{\partial t}\right]\phi_c(\mathbf{r},t), \quad (22)$$

where we have resurrected time arguments for clarity. As in the zeroth-order GPE case—where it was possible, and convenient for the case of a stationary, equilibrium initial state, to replace the time-dependent GPE eigenvalue $\lambda_0^{(0)}(t)$ with a time-independent GPE eigenvalue $\lambda_0^{(0)}$—$\bar{\lambda}_0(t)$ is an explicitly real quantity. It will thus later be convenient, for the case of a stationary, equilibrium initial state, to replace the time-dependent "GPE eigenvalue" $\lambda_0^{(2)}(t)$ with the time-independent "GPE eigenvalue" $\lambda_0^{(2)}$ given by

$$\lambda_0^{(2)} = \int d\mathbf{r}\phi_c^*(\mathbf{r},0)[H_{\rm sp}(\mathbf{r},0) + \tilde{U}|\phi_c(\mathbf{r},0)|^2]\phi_c(\mathbf{r},0). \quad (23)$$

Note, however, that the replacement of $\lambda_0^{(2)}(t)$ with $\lambda_0^{(2)}$ must be accomplished consistently with the replacement of $\lambda_2^{(2)}(t)$ with a real, time-independent quantity as discussed previously. The details of this consistent replacement are outlined in Sec. III.

The generalized Gross-Pitaevskii equation [Eq. (14)] and the modified Bogoliubov–de Gennes equations [Eq. (19)] complete the fully dynamical, second-order, number-conserving description obtained by Gardiner and Morgan in Ref. [51] and previously used within a linear response treatment by Morgan [59–61]. In this paper, we develop these equations into a form where their fully dynamical time evolution can be realized numerically, as in Ref. [41].

C. Discussion

Before we outline our method for the simultaneous numerical solution of Eqs. (14) and (19), a few comments regarding the properties of the second-order equations of motion and their regime of validity are in order. Firstly we note that, in general, the diagonal part of the anomalous average, $\tilde{m}(\mathbf{r},\mathbf{r})$, is ultraviolet divergent and must be appropriately renormalized; this procedure is described in detail in Refs. [51] and [56]. One exception is in the case of quasi-one-dimensional (quasi-1D) systems, such as the one we consider in Sec. IV, where renormalization is not necessary.

Secondly, the number-conserving equations of motion used here are derived by expanding the total Hamiltonian in powers of the number-conserving fluctuation operator $\tilde{\Lambda}(\mathbf{r})$ [Eq. (17)]. This operator is advantageous for three primary reasons: (1) It scales proportionally to the number of noncondensate atoms, which we wish to treat as a small parameter; (2) it avoids the need to expand inverse-square-root number operators when expanding the Hamiltonian, which is particularly convenient; and (3) it is a well-defined fluctuation operator in the sense that $\langle\tilde{\Lambda}(\mathbf{r},t)\rangle = 0$. It should be noted that the commutation relations of $\tilde{\Lambda}(\mathbf{r})$,

$$[\tilde{\Lambda}(\mathbf{r}),\tilde{\Lambda}^\dagger(\mathbf{r}')] = \frac{\hat{N}_c}{N_c}\mathcal{Q}(\mathbf{r},\mathbf{r}') - \frac{1}{N_c}\delta\hat{\Psi}^\dagger(\mathbf{r}')\delta\hat{\Psi}(\mathbf{r}), \quad (24)$$

give rise to quasiparticles which are, in principle, only approximately bosonic. However, when restricted to the (quadratic) order of approximation we consider, the corresponding quasiparticles are indeed exactly bosonic. Hence, the favorable properties of $\tilde{\Lambda}(\mathbf{r})$ mentioned above make it a preferable choice for developing the second-order equations of motion [51,56,59–61,66].

Note also that the appearance of higher-than-second-order fluctuation terms in the equations of motion has been prevented by working within a consistent Gaussian approximation [51]; that is, all *quadratic* products of operators are required to take the form of pair averages. This constitutes a Gaussian approximation in that all higher-order moments of the fluctuation distribution are assumed to be describable in terms of $\langle\tilde{\Lambda}^\dagger(\mathbf{r})\tilde{\Lambda}(\mathbf{r})\rangle$ and $\langle\tilde{\Lambda}(\mathbf{r})\tilde{\Lambda}(\mathbf{r})\rangle$ [67]. As was explicitly demonstrated by Morgan [56] this is consistent within the second-order number-conserving description (see also Refs. [2,51]).

A key property of the second-order number-conserving equations of motion is their *number self-consistency*: in contrast to $\lambda_0^{(0)}$ and $\lambda_0^{(2)}$—which can both be considered as low-order approximations to the chemical potential—$\lambda_2^{(2)}(t)$ is a *complex* eigenvalue. The meaning of the imaginary part of $\lambda_2^{(2)}(t)$ can be understood by considering the (implicit) time dependence of N_c, which is given (to quadratic order) by

$$\begin{aligned} i\hbar\frac{dN_c}{dt} &= i\hbar\frac{d}{dt}\left[N - \int d\mathbf{r}\langle\tilde{\Lambda}^\dagger(\mathbf{r})\tilde{\Lambda}(\mathbf{r})\rangle\right], \\ &= -\int d\mathbf{r}\left\{\left\langle\tilde{\Lambda}^\dagger(\mathbf{r})\left[i\hbar\frac{d}{dt}\tilde{\Lambda}(\mathbf{r})\right]\right\rangle \right. \\ &\quad \left. + \left\langle\left[i\hbar\frac{d}{dt}\tilde{\Lambda}^\dagger(\mathbf{r})\right]\tilde{\Lambda}(\mathbf{r})\right\rangle\right\}, \\ &= \tilde{U}\int d\mathbf{r}[\phi_c^*(\mathbf{r})^2\tilde{m}(\mathbf{r},\mathbf{r}) - \tilde{m}^*(\mathbf{r},\mathbf{r})\phi_c(\mathbf{r})^2], \\ &= \left[\lambda_2^{(2)}(t) - \lambda_2^{(2)*}(t)\right]N_c. \end{aligned} \quad (25)$$

Thus the time-dependent, imaginary part of $\lambda_2^{(2)}(t)$ acts to keep the condensate mode $\phi_c(\mathbf{r})$ normalized to unity despite the growth or decay of the condensate population. This illustrates the presence of number self-consistency in the dynamical coupling between the GGPE and MBdGE. In contrast, the first-order description [52,53]—which consists of the same MBdGE [Eq. (19)] coupled to the ordinary GPE [Eq. (11)]—is *not* in general number self-consistent, since the condensate population is fixed. The first-order description can only be considered to be number self-consistent when viewed as the limit of the second-order description as $N \to \infty$ [51]. The zeroth-order description, consisting of the GPE [Eq. (11)] alone,

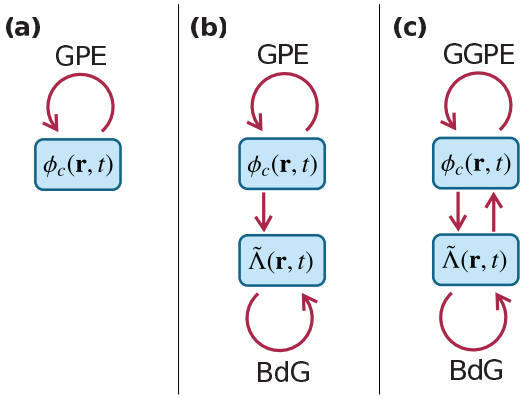

FIG. 1. (Color online) Schematic representation of the zeroth-, first-, and second-order number-conserving equations of motion. At zeroth order, (a), the noncondensate is ignored and the condensate mode $\phi_c^{(0)}(\mathbf{r})$ is described by the Gross-Pitaevskii equation (GPE) [Eq. (11)]. At first order, (b), the GPE [Eq. (11)] is coupled to modified Bogoliubov–de Gennes equations (MBdGE) [Eq. (19)] for the noncondensate fluctuation operator $\tilde{\Lambda}(\mathbf{r})$. At this order, the evolution of $\tilde{\Lambda}(\mathbf{r})$ depends on the evolution of $\phi_c^{(0)}(\mathbf{r})$, but the converse is not true; this order of approximation can be interpreted as treating the condensate as an infinite atomic reservoir. At second order, (c), the noncondensate is again described by the MBdGE [Eq. (19)]; however, the evolution of the condensate mode $\phi_c(\mathbf{r})$ is now determined by the generalized Gross-Pitaevskii equation (GGPE) [Eq. (14)]. This pairing of equations produces fully self-consistent number dynamics.

is trivially number self-consistent, as it ignores the growth and decay of the condensate altogether. The number self-consistency of the zero-, first-, and second-order number-conserving descriptions are illustrated schematically in Fig. 1.

A final feature of the second-order, number-conserving equations of motion is that the noncondensate is described by a MBdGE [Eq. (19)] which does not contain pair averages of the noncondensate operators; the terms $\mathcal{M}(\mathbf{r},\mathbf{r}')$ are in no way altered from the first-order description and the terms $\mathcal{L}(\mathbf{r},\mathbf{r}')$ appearing in the MBdGE consist only of a GPE Hamiltonian and the "GPE eigenvalue" of Eq. (23). Importantly, however, the GPE Hamiltonian and the "GPE eigenvalue" are, in the second-order description, evaluated in terms of the second-order GGPE wave function $\phi_c(\mathbf{r})$. This leads to an apparent inconsistency in that the spinors $[\phi_c(\mathbf{r}),0]^T$ and $[0,\phi_c^*(\mathbf{r})]^T$ are no longer exact, zero-energy solutions of the MBdGE, as they would be for the GPE wave function $\phi_c^{(0)}$. This has the unfortunate side effect of making the identification of self-consistent initial conditions difficult at high temperatures, particularly in inhomogeneous systems. However, this problem can be viewed purely as a consequence of applying the theory outside of its regime of validity, as argued by Morgan in his study of condensate excitations at finite temperature [59–61]; in this work he demonstrated that the second-order description remains self-consistent at high temperatures (approaching $N_t \sim N_c$) provided one restricts oneself to a linear response treatment, in which a self-consistent equilibrium solution is not necessary. A fully dynamical treatment, which requires a self-consistent equilibrium initial condition, is thus restricted to lower temperatures (such that $N_t < N_c$) than a linear response treatment.

III. FULLY TIME-DEPENDENT NUMERICAL IMPLEMENTATION

A. Reformulation of equations of motion

1. Elimination of complex, time-dependent "eigenvalue"

In this section we develop a numerical method for evolving the combined GGPE and MBdGE system of Eqs. (14) and (19). In order to do so, it is of great convenience to eliminate the imaginary part of the GGPE "eigenvalue" $\lambda_2^{(2)}(t)$ [Eq. (18)]; this can be done by describing the condensate using a mode function normalized to the condensate population, N_c. Hence, we define

$$\psi(\mathbf{r}) = \sqrt{N_c}\phi_c(\mathbf{r}), \tag{26}$$

in terms of which the GGPE can be re-expressed [using Eq. (25) for the number evolution] as

$$\begin{aligned} i\hbar\frac{\partial\psi(\mathbf{r})}{\partial t} &= \left[H_{\rm sp}(\mathbf{r}) + U_0|\psi(\mathbf{r})|^2 - \bar{\lambda}_2^{(2)}\right]\psi(\mathbf{r}) \\ &\quad + U_0\left[\tilde{n}(\mathbf{r},\mathbf{r}) - \frac{|\psi(\mathbf{r})|^2}{N_c}\right]\psi(\mathbf{r}) \\ &\quad + U_0\tilde{n}(\mathbf{r},\mathbf{r})\psi(\mathbf{r}) - \frac{U_0}{N_c}\int d\mathbf{r}'\psi(\mathbf{r}')|\psi(\mathbf{r}')|^2\tilde{n}(\mathbf{r},\mathbf{r}') \\ &\quad + U_0\tilde{m}(\mathbf{r},\mathbf{r})\psi^*(\mathbf{r}) - \frac{U_0}{N_c}\int d\mathbf{r}'\psi^*(\mathbf{r}') \\ &\quad \times|\psi(\mathbf{r}')|^2\tilde{m}(\mathbf{r},\mathbf{r}'), \end{aligned} \tag{27}$$

where the adjusted GGPE eigenvalue, $\bar{\lambda}_2^{(2)} = \mathrm{Re}(\lambda_2^{(2)})$, is given by

$$\begin{aligned} \bar{\lambda}_2^{(2)} = \lambda_0^{(2)} + \frac{U_0}{N_c}\int d\mathbf{r}\left\{\psi^*(\mathbf{r})\left[2\tilde{n}(\mathbf{r},\mathbf{r}) - \frac{1}{N_c}|\psi(\mathbf{r})|^2\right]\psi(\mathbf{r})\right. \\ \left. + \frac{U_0}{2N_c}[\psi(\mathbf{r})^{*2}\tilde{m}(\mathbf{r},\mathbf{r}) + \psi(\mathbf{r})^2\tilde{m}^*(\mathbf{r},\mathbf{r})]\right\}. \end{aligned} \tag{28}$$

This is explicitly real, and should be evaluated explicitly in terms of the stationary, equilibrium initial condition of the GGPE at $t = 0$.

Note that in order to cast the GGPE in the above form, with time-independent eigenvalue $\bar{\lambda}_2^{(2)}$, we have formally moved into a frame which cancels the time dependence of the *real* part of $\lambda_2^{(2)}(t)$. However, transforming the MBdGE into the same frame leads to additional terms of the form $\delta(\mathbf{r}-\mathbf{r}')[f(t=0) - f(t)]$ (where $t = 0$ refers to the equilibrium initial condition) appearing in the operator $\mathcal{L}(\mathbf{r},\mathbf{r}')$. Specifically, such terms appear with

$$\begin{aligned} f(t) = \frac{U_0}{N_c}\int d\mathbf{r}\left\{\psi^*(\mathbf{r})\left[2\tilde{n}(\mathbf{r},\mathbf{r}) - \frac{1}{N_c}|\psi(\mathbf{r})|^2\right]\psi(\mathbf{r})\right. \\ \left. + \frac{U_0}{2N_c}[\psi(\mathbf{r})^{*2}\tilde{m}(\mathbf{r},\mathbf{r}) + \psi(\mathbf{r})^2\tilde{m}^*(\mathbf{r},\mathbf{r})]\right\}, \end{aligned} \tag{29}$$

where all quantities except U_0 on the right-hand side are time dependent. Since these terms are small, and formally of the same (cubic) order with respect to the fluctuation operator $\tilde{\Lambda}(\mathbf{r})$ as terms already omitted from the description of the noncondensate at second order [51], they should be neglected to maintain a consistent description. We thus cast the MBdGE

as

$$
\begin{aligned}
&i\hbar\frac{\partial}{\partial t}\tilde{\Lambda}(\mathbf{r})\\
&\quad=\left[H_{\rm sp}(\mathbf{r})+U_0|\psi(\mathbf{r})|^2-\lambda_0^{(2)}\right]\tilde{\Lambda}(\mathbf{r})\\
&\qquad+U_0|\psi(\mathbf{r})|^2\tilde{\Lambda}(\mathbf{r})-\frac{U_0}{N_c}\int d\mathbf{r}'\psi^*(\mathbf{r}')|\psi(\mathbf{r}')|^2\tilde{\Lambda}(\mathbf{r}')\psi(\mathbf{r})\\
&\qquad+U_0\psi(\mathbf{r})^2\tilde{\Lambda}^\dagger(\mathbf{r})-\frac{U_0}{N_c}\int d\mathbf{r}'\psi(\mathbf{r}')|\psi(\mathbf{r}')|^2\tilde{\Lambda}^\dagger(\mathbf{r}')\psi(\mathbf{r}),
\end{aligned}
\tag{30}
$$

a form which emphasizes the significant structural analogies between the GGPE and MBdGE.

2. *Quasiparticle decomposition*

In numerical studies of nonequilibrium dynamics at finite temperature one generally wishes to begin from a finite-temperature equilibrium condition and explore the dynamics resulting from, e.g., driving or an abrupt quench event in a fully time-dependent way[2]. In the second-order number-conserving description such a thermal and dynamical equilibrium state corresponds to a self-consistent, stationary solution of the equations of motion in which the elementary quasiparticle excitations of the system are populated according to the appropriate thermal Bose distribution.

The appropriate quasiparticle basis in the second-order number-conserving description is the basis of Bogoliubov quasiparticle modes which diagonalize the stationary MBdGE [51]:

$$
\begin{aligned}
&\begin{pmatrix}\mathcal{L}(\mathbf{r},\mathbf{r}') & \mathcal{M}(\mathbf{r},\mathbf{r}')\\ -\mathcal{M}^*(\mathbf{r},\mathbf{r}') & -\mathcal{L}^*(\mathbf{r},\mathbf{r}')\end{pmatrix}\\
&\quad=\sum_{k=1}^{\infty}\epsilon_k\begin{pmatrix}u_k(\mathbf{r})\\ v_k(\mathbf{r})\end{pmatrix}(u_k^*(\mathbf{r}'),-v_k^*(\mathbf{r}'))\\
&\qquad-\sum_{k=1}^{\infty}\epsilon_k\begin{pmatrix}v_k^*(\mathbf{r})\\ u_k^*(\mathbf{r})\end{pmatrix}(-v_k(\mathbf{r}'),u_k(\mathbf{r}')).
\end{aligned}
\tag{31}
$$

In terms of the quasiparticle mode functions $u_k(\mathbf{r})$ and $v_k(\mathbf{r})$, the fluctuation operator $\tilde{\Lambda}(\mathbf{r})$ can be expanded as

$$
\begin{pmatrix}\tilde{\Lambda}(\mathbf{r})\\ \tilde{\Lambda}^\dagger(\mathbf{r})\end{pmatrix}=\sum_{k=1}^{\infty}\tilde{b}_k\begin{pmatrix}u_k(\mathbf{r})\\ v_k(\mathbf{r})\end{pmatrix}+\sum_{k=1}^{\infty}\tilde{b}_k^\dagger\begin{pmatrix}v_k^*(\mathbf{r})\\ u_k^*(\mathbf{r})\end{pmatrix},
\tag{32}
$$

where $\tilde{b}_k^\dagger$ and $\tilde{b}_k$ are quasiparticle creation and annihilation operators which, at this order, are assumed to have bosonic commutation relations (see Sec. II C). Assuming all time dependence to reside in the quasiparticle mode functions $u_k(\mathbf{r})$ and $v_k(\mathbf{r})$, with the quasiparticle creation and annihilation operators $\tilde{b}_k^\dagger$ and $\tilde{b}_k$ time independent, the MBdGE [Eq. (30)] take the form,

$$
\begin{aligned}
&i\hbar\frac{\partial}{\partial t}u_k(\mathbf{r})\\
&\quad=\left[H_{\rm sp}(\mathbf{r})+U_0|\psi(\mathbf{r})|^2-\lambda_0^{(2)}\right]u_k(\mathbf{r})\\
&\qquad+U_0|\psi(\mathbf{r})|^2u_k(\mathbf{r})-\frac{U_0}{N_c}\int d\mathbf{r}'\psi^*(\mathbf{r}')|\psi(\mathbf{r}')|^2u_k(\mathbf{r}')\psi(\mathbf{r})\\
&\qquad+U_0\psi(\mathbf{r})^2v_k(\mathbf{r})-\frac{U_0}{N_c}\int d\mathbf{r}'\psi(\mathbf{r}')|\psi(\mathbf{r}')|^2v_k(\mathbf{r}')\psi(\mathbf{r}),
\end{aligned}
\tag{33}
$$

and

$$
\begin{aligned}
&i\hbar\frac{\partial}{\partial t}v_k^*(\mathbf{r})\\
&\quad=\left[H_{\rm sp}(\mathbf{r})+U_0|\psi(\mathbf{r})|^2-\lambda_0^{(2)}\right]v_k^*(\mathbf{r})\\
&\qquad+U_0|\psi(\mathbf{r})|^2v_k^*(\mathbf{r})-\frac{U_0}{N_c}\int d\mathbf{r}'\psi^*(\mathbf{r}')|\psi(\mathbf{r}')|^2v_k^*(\mathbf{r}')\psi(\mathbf{r})\\
&\qquad+U_0\psi(\mathbf{r})^2u_k^*(\mathbf{r})-\frac{U_0}{N_c}\int d\mathbf{r}'\psi(\mathbf{r}')|\psi(\mathbf{r}')|^2u_k^*(\mathbf{r}')\psi(\mathbf{r}).
\end{aligned}
\tag{34}
$$

At initial thermal equilibrium, the quasiparticle creation and annihilation operators have the following pair averages:

$$
\langle\tilde{b}_k^\dagger\tilde{b}_l\rangle=\delta_{kl}N_k,
\tag{35}
$$

$$
\langle\tilde{b}_k\tilde{b}_l\rangle=\langle\tilde{b}_k^\dagger\tilde{b}_l^\dagger\rangle=0,
\tag{36}
$$

where N_k is the Bose-Einstein factor [51,56,60],

$$
N_k=\left[\exp\left(\frac{\epsilon_k-\left[\mu-\lambda_0^{(2)}\right]}{k_BT}\right)-1\right]^{-1}.
\tag{37}
$$

The term $\mu-\lambda_0^{(2)}$ represents a finite-size correction, given by Refs. [56,60,68]

$$
\mu-\lambda_0^{(2)}=-k_BT\ln\left(1-N_c^{-1}\right).
\tag{38}
$$

This leads to quasiparticle expressions for the noncondensate normal and anomalous averages [Eqs. (15) and (16)]:

$$
\tilde{n}(\mathbf{r},\mathbf{r}')=\sum_{k=1}^{\infty}N_ku_k(\mathbf{r})u_k^*(\mathbf{r}')+\sum_{k=1}^{\infty}(N_k+1)v_k^*(\mathbf{r})v_k(\mathbf{r}'),
\tag{39}
$$

$$
\tilde{m}(\mathbf{r},\mathbf{r}')=\sum_{k=1}^{\infty}N_ku_k(\mathbf{r})v_k^*(\mathbf{r}')+\sum_{k=1}^{\infty}(N_k+1)v_k^*(\mathbf{r})u_k(\mathbf{r}').
\tag{40}
$$

We reiterate that, by choosing a scheme where all time dependence resides in the quasiparticle mode functions $u_k(\mathbf{r})$ and $v_k(\mathbf{r})$, the quasiparticle populations N_k appearing in Eqs. (39) and (40) remain *fixed* in time.

Using the above expressions we proceed, in the next section, to recast the GGPE in terms of the quasiparticle mode functions, and recast the combined GGPE and MBdGE—now in the form of Eqs. (27), (33), and (34)—in the final form which we will use to conduct a simultaneous numerical solution.

[2]One could in principle start from a nonequilibrium initial condition, but we consider only the equilibrium case here.

3. *Introduction of the spinor ζ*

The primary difficultly in simulating the coupled GGPE-MBdGE system numerically is the problem of orthogonalization: *both* equations contain terms which function to maintain orthogonality between the condensate and noncondensate. This is in contrast to the case of the first-order GPE-MBdGE system, where the GPE evolves in isolation from the MBdGE; this de-coupling in the first-order system means the evolution of the MBdGE can be computed by *ignoring* the projector terms in the MBdGE throughout the evolution, and simply projecting the final state orthogonally to the condensate [35]. However, if one were to similarly ignore the projectors during the evolution of the second-order GGPE-MBdGE system, one would then have to reorthogonalize both the condensate and quasiparticle modes with respect to an *unknown* basis at the end of the evolution. Consequently, the projection terms, and the nonlocal integrals they involve, must be explicitly included in any numerical method. In this section we develop such a method, by re-casting the GGPE and MBdGE in a form which exploits their apparent symmetries, and allows us to include the projection terms using a split-step technique.

After substituting the quasiparticle expressions for the normal and anomalous average [Eqs. (39) and (40)] into the GGPE [Eq. (27)], the GGPE can be recast in the form,

$$i\hbar\frac{\partial\psi(\mathbf{r})}{\partial t} = [H_{\rm GP}(\mathbf{r}) + B(\mathbf{r})]\,\psi(\mathbf{r}) + \sum_{k=1}^{\infty}(N_k+1)A_k(\mathbf{r})v_k^*(\mathbf{r}) + \sum_{k=1}^{\infty}N_kA_k^*(\mathbf{r})u_k(\mathbf{r}), \tag{41}$$

and the MBdGE [Eqs. (33) and (34)] can be recast in the form,

$$i\hbar\frac{\partial u_k(\mathbf{r})}{\partial t} = H_{\rm GP}(\mathbf{r})u_k(\mathbf{r}) + A_k(\mathbf{r})\psi(\mathbf{r}), \tag{42}$$

$$i\hbar\frac{\partial v_k^*(\mathbf{r})}{\partial t} = H_{\rm GP}(\mathbf{r})v_k^*(\mathbf{r}) + A_k^*(\mathbf{r})\psi(\mathbf{r}), \tag{43}$$

where

$$H_{\rm GP}(\mathbf{r}) = H_{\rm sp}(\mathbf{r}) + U_0|\psi(\mathbf{r})|^2 - \lambda_0^{(2)}, \tag{44}$$

$$A_k(\mathbf{r}) = U_0[v_k(\mathbf{r})\psi(\mathbf{r}) + u_k(\mathbf{r})\psi^*(\mathbf{r}) - I_k], \tag{45}$$

$$I_k = \frac{1}{N_c}\int d\mathbf{r}[v_k(\mathbf{r})\psi(\mathbf{r}) + u_k(\mathbf{r})\psi^*(\mathbf{r})]|\psi(\mathbf{r})|^2, \tag{46}$$

and

$$B(\mathbf{r}) = U_0\left[\sum_{k=1}^{\infty}N_k|u_k(\mathbf{r})|^2 + (N_k+1)|v_k(\mathbf{r})|^2\right] - U_0\frac{|\psi(\mathbf{r})|^2}{N_c} - \lambda', \tag{47}$$

where $\lambda' = \bar{\lambda}_2^{(2)} - \lambda_0^{(2)}$. This reformulation of the problem allows one to write the coupled evolution of the condensate wave function and the first M quasiparticle modes as a nonlinear matrix equation in a $(2M+1)$-dimensional spinor space:

$$i\hbar\frac{\partial}{\partial t}\zeta(\mathbf{r}) = \Gamma(\mathbf{r})\zeta(\mathbf{r}). \tag{48}$$

Here the vector $\zeta(\mathbf{r})$ is defined by

$$\zeta(\mathbf{r}) = [\psi(\mathbf{r}), v_1^*(\mathbf{r}), \ldots, v_M^*(\mathbf{r}), u_1(\mathbf{r}), \ldots, u_M(\mathbf{r})]^T, \tag{49}$$

and the operator $\Gamma(\mathbf{r})$ is defined by

$$\Gamma(\mathbf{r}) = \begin{pmatrix} H_{\rm GP}(\mathbf{r})+B(\mathbf{r}) & (N_1+1)A_1(\mathbf{r}) & (N_2+1)A_2(\mathbf{r}) & \cdots & (N_M+1)A_M(\mathbf{r}) & N_1A_1^*(\mathbf{r}) & N_2A_2^*(\mathbf{r}) & \cdots & N_MA_M^*(\mathbf{r}) \\ A_1^*(\mathbf{r}) & H_{\rm GP}(\mathbf{r}) & 0 & \cdots & 0 & 0 & 0 & \cdots & 0 \\ A_2^*(\mathbf{r}) & 0 & H_{\rm GP}(\mathbf{r}) & \cdots & 0 & 0 & 0 & \cdots & 0 \\ \vdots & \vdots & \vdots & \ddots & \vdots & \vdots & \vdots & \cdots & \vdots \\ A_M^*(\mathbf{r}) & 0 & 0 & \cdots & H_{\rm GP}(\mathbf{r}) & 0 & 0 & \cdots & 0 \\ A_1(\mathbf{r}) & 0 & 0 & \cdots & 0 & H_{\rm GP}(\mathbf{r}) & 0 & \cdots & 0 \\ A_2(\mathbf{r}) & 0 & 0 & \cdots & 0 & 0 & H_{\rm GP}(\mathbf{r}) & \cdots & 0 \\ \vdots & \vdots & \vdots & \vdots & \vdots & \vdots & \vdots & \ddots & \vdots \\ A_M(\mathbf{r}) & 0 & 0 & \cdots & 0 & 0 & 0 & \cdots & H_{\rm GP}(\mathbf{r}) \end{pmatrix}. \tag{50}$$

In any actual calculation, this spinor space is rendered finite dimensional by the need for a finite quasiparticle momentum cutoff M. However, M may, in principle, be arbitrarily large.

B. Operator-splitting scheme for time evolution

1. *Separation of position and momentum terms*

As we have already accounted for all creation and annihilation operators through the quasiparticle decomposition, each entry in the matrix defining $\Gamma(\mathbf{r})$ can be thought of as an operator in the first-quantized sense.[3] From an analytic perspective, this notation seems to achieve little more than "tidying"—abstracting away much of the detail. Importantly, however, all the operators which are off-diagonal in the spinor

[3]That is, an operator which could appear on the right side of a *single-particle* Schrödinger equation.

space [the operators $A_k(\mathbf{r})$] are diagonal in the position representation, since they ultimately consist of a multiplication by a spatially varying function. In contrast, all the operators which have off-diagonal components in the position representation [that is, the kinetic energy operator implicitly contained in $H_{\rm sp}(\mathbf{r})$ and hence in $H_{\rm GP}(\mathbf{r})$] appear only on the diagonal in the spinor space.

From a numerical perspective this arrangement is extremely useful, as it makes the evolution amenable to a split-step approximation. This is achieved by splitting $\Gamma(\mathbf{r})$ into the sum of a term representing the linear single-particle evolution $\Gamma_{\rm L}(\mathbf{r})$, and a term representing nonlinear parts of the evolution, $\Gamma_{\rm N}(\mathbf{r})$. The linear, single-particle term is defined by

$$\Gamma_{\rm L}(\mathbf{r}) = I \otimes H_{\rm L}(\mathbf{r}), \tag{51}$$

where I represents the $(2M+1)\times(2M+1)$ identity matrix, and we have also defined

$$H_{\rm L}(\mathbf{r}) = H_{\rm sp}(\mathbf{r}) - \lambda_0^{(2)}. \tag{52}$$

The nonlinear term is then defined simply by

$$\Gamma_{\rm N}(\mathbf{r}) = \Gamma(\mathbf{r}) - \Gamma_{\rm L}(\mathbf{r}). \tag{53}$$

Note that this matrix contains diagonal entries of the form $H_{\rm N}(\mathbf{r})$ and $H_{\rm N}(\mathbf{r}) + B(\mathbf{r})$ where

$$H_{\rm N}(\mathbf{r}) = H_{\rm GP}(\mathbf{r}) - H_{\rm L}(\mathbf{r}). \tag{54}$$

Written in this form, $\Gamma_{\rm L}(\mathbf{r})$ contains all kinetic energy terms; while these terms are not diagonal in the position representation, they do all lie on the diagonal in the spinor space. Consequently, the evolution due to the kinetic energy terms can be computed for each mode function *separately*. In contrast, while $\Gamma_{\rm N}(\mathbf{r})$ does contain off-diagonal elements in the spinor space, each element of $\Gamma_{\rm N}(\mathbf{r})$ is diagonal in the position representation. Consequently, the evolution due to these terms can be computed straightforwardly over a discrete spatial grid.

In the spinor space, the split-step approximation for the evolution of the system over short times δt is given by

$$\begin{aligned}\zeta(\mathbf{r},t+\delta t) &= e^{-i\Gamma(\mathbf{r})\delta t/\hbar}\zeta(\mathbf{r},t)\\ &\approx e^{-i\Gamma_{\rm N}(\mathbf{r})\delta t/2\hbar}e^{-i\Gamma_{\rm L}(\mathbf{r})\delta t/\hbar}e^{-i\Gamma_{\rm N}(\mathbf{r})\delta t/\hbar}\zeta(\mathbf{r},t),\end{aligned} \tag{55}$$

where each of the three evolution operators on the right is assumed to act instantaneously, and the symmetrization reduces the error to the order of δt^3 [69]. Since $\Gamma_{\rm L}(\mathbf{r})$ is diagonal in the spinor space, we have

$$e^{-i\Gamma_{\rm L}(\mathbf{r})\delta t/\hbar} = I \otimes e^{-iH_{\rm L}(\mathbf{r})\delta t/\hbar}. \tag{56}$$

2. Analytic form for position-space evolution

The spatial operator $\Gamma_{\rm N}(\mathbf{r})$ is more problematic because it is not diagonal in the spinor space, and because it contains the nonlocal, nonlinear terms necessary to preserve orthogonality between the condensate and noncondensate. However, each of its entries *is* diagonal in the position representation, meaning we only need exponentiate $\Gamma_{\rm N}(\mathbf{r})$ in the spinor space in order to obtain an operator we can evaluate and use for short-time propagation *at a given position*: such an operator—in distinct contrast to $e^{-i\Gamma_{\rm L}(\mathbf{r})\delta t/\hbar}$ which consists of an application of $e^{-iH_{\rm L}(\mathbf{r})\delta t/\hbar}$ to each mode *individually*—*couples* the mode functions by acting on *all modes at once*. The numerical advantage of casting the evolution in terms of such an operator is that it almost entirely overcomes the problem of retaining orthogonality between the condensate and the quasiparticle modes, which poses severe difficulties for other schemes. In practice we do find that a correction for numerical round-off error is still required in order to preserve complete orthogonality over long times; this can be achieved by explicitly orthogonalizing the quasiparticle modes with respect to the condensate at the end of each time step. However, our experience is that applying such a correction after every time step does not cause decay of the total atom number, indicating that the need for such a correction does indeed stem from the numerical round-off error inherent in finite-precision arithmetic. Indeed, the problem of loss of orthogonality between vectors due to finite-precision arithmetic is well known in the context of, e.g., the Gram-Schmidt process [70].

In principle, the evolution due to the term $e^{-i\Gamma_{\rm N}(\mathbf{r})\delta t/2\hbar}$ can be obtained, for a given $\mathbf{r}$, by exponentiating the matrix $\Gamma_{\rm N}(\mathbf{r})$ numerically at each spatial grid point. However, with the necessary number of floating point operations necessary to diagonalize the matrix $\Gamma_{\rm N}(\mathbf{r})$ scaling at least as $(2M+1)^3$ [70], this leads to an algorithm which is too slow to be practicable. To overcome this limitation, we have computed a general analytic expression for $e^{-i\Gamma_{\rm N}(\mathbf{r})\delta t/2\hbar}$ for arbitrary M: this reduces the scaling of the computational effort to $(2M+1)^2$ (i.e., equivalent to a matrix-vector multiplication). This expression is explicitly derived in Appendix, where we also show that, at any specific point $\mathbf{r}$ (and time t) on the computational grid, the time evolution due to $\Gamma_{\rm N}$ can be approximated locally, after numerical evaluation of the nonlocal integrals appearing in the functions $A_k(\mathbf{r})$ over the entire position-space grid, by the following $2M+1$ coupled equations:

$$\begin{aligned}\psi(\mathbf{r},t+\delta t/2) = &\left(T_{\cos}(\mathbf{r},t) - \tfrac{1}{2}T_{\sin}(\mathbf{r},t)B(\mathbf{r},t)\right)\psi(\mathbf{r},t)\\ &- T_{\sin}(\mathbf{r},t)\Xi(\mathbf{r},t),\end{aligned} \tag{57}$$

$$\begin{aligned}v_k^*(\mathbf{r},t+\delta t/2) = &-A_k^*(\mathbf{r},t)T_{\sin}(\mathbf{r},t)\psi(\mathbf{r},t) + T_{\exp}(\mathbf{r},t)v_k^*(\mathbf{r},t)\\ &+ A_k^*(\mathbf{r},t)T_{\rm mix}(\mathbf{r},t)\Xi(\mathbf{r},t),\end{aligned} \tag{58}$$

$$\begin{aligned}u_k(\mathbf{r},t+\delta t/2) = &-A_k(\mathbf{r},t)T_{\sin}(\mathbf{r},t)\psi(\mathbf{r},t) + T_{\exp}(\mathbf{r},t)u_k(\mathbf{r},t)\\ &+ A_k(\mathbf{r},t)T_{\rm mix}(\mathbf{r},t)\Xi(\mathbf{r},t),\end{aligned} \tag{59}$$

where

$$\Xi(\mathbf{r},t) = \sum_{l=1}^{M}(N_l+1)A_l(\mathbf{r},t)v_l^*(\mathbf{r},t) + N_l A_l^*(\mathbf{r},t)u_l(\mathbf{r},t), \tag{60}$$

and we have defined

$$T_{\exp}(\mathbf{r},t) = \exp\left(\frac{-iH_{\rm N}(\mathbf{r},t)\delta t}{2\hbar}\right), \tag{61}$$

$$\begin{aligned}T_{\cos}(\mathbf{r},t) = &\exp\left[\frac{-i\left(H_{\rm N}(\mathbf{r},t)+\frac{1}{2}B(\mathbf{r},t)\right)\delta t}{2\hbar}\right]\\ &\times\cos\left\{\left[\left(\frac{B(\mathbf{r},t)}{2}\right)^2+\Sigma(\mathbf{r},t)\right]^{\frac{1}{2}}\frac{\delta t}{2\hbar}\right\},\end{aligned} \tag{62}$$

$$T_{\sin}(\mathbf{r},t) = \exp\left[\frac{-i\left(H_{\mathrm{N}}(\mathbf{r},t) + \frac{1}{2}B(\mathbf{r},t)\right)\delta t}{2\hbar}\right] \times \frac{i\sin\left\{\left[\left(\frac{B(\mathbf{r},t)}{2}\right)^2 + \Sigma(\mathbf{r},t)\right]^{\frac{1}{2}}\frac{\delta t}{2\hbar}\right\}}{\left[\left(\frac{B(\mathbf{r},t)}{2}\right)^2 + \Sigma(\mathbf{r},t)\right]^{\frac{1}{2}}}, \quad (63)$$

$$T_{\mathrm{mix}}(\mathbf{r},t) = \frac{T_{\cos}(\mathbf{r},t) + \frac{1}{2}T_{\sin}(\mathbf{r},t)B(\mathbf{r},t) - T_{\exp}(\mathbf{r},t)}{\Sigma(\mathbf{r},t)}, \quad (64)$$

and

$$\Sigma(\mathbf{r},t) = \sum_{k=1}^{M}(2N_k + 1)|A_k(\mathbf{r},t)|^2. \quad (65)$$

Note that the quasiparticle index k in Eqs. (58) and (59) runs from 1 to M, and we have chosen to show time dependencies explicitly in Eqs. (57)–(59), to make the time-dependent nature of the expression clear. The analytic evolution scheme given by Eqs. (57)–(59), incorporated into the symmetrized split-step method of Eq. (55), provides a way to numerically implement the second-order number-conserving description of Sec. II.

IV. NONEQUILIBRIUM DYNAMICS OF THE δ-KICKED-ROTOR BEC AT FINITE TEMPERATURES

A. Overview

In this section we apply the split-step numerical method developed in the previous section for evolving the second-order, number-conserving equations of motion—consisting of coupled GGPE and MBdGE—to the δ-kicked-rotor BEC. This system consists of a quasi-1D, toroidally trapped, repulsively interacting atomic BEC driven by δ kicks from a spatial cosine potential, and serves as a prototypical example of a system where condensate depletion occurs dynamically as a result of external driving. The free parameters of this system can be expressed in terms of dimensionless kick strength κ, kick period T_p, and interaction strength g_T, plus the total atom number N, as shown in Fig. 2 (see Sec. IV B for a full definition of these parameters). This system is a BEC analog of the quantum δ-kicked rotor [71–75], a paradigm quantum-chaotic system exhibiting complex behavior as a result of the periodic driving [71,72,75]. In particular, the δ-kicked rotor exhibits quantum resonant driving frequencies, which occur whenever the kick period T_p is a rational fraction of the Talbot time $T_p = 4\pi$. At these frequencies the uptake of energy from the driving potential is greatly increased, with diffusive (linear in time) expansion of the state in momentum space being replaced by ballistic (quadratic in time) expansion at resonance [71–73]. Such systems have previously been realized in the context of atom-optics experiments [74–77]. However, the δ-kicked-rotor BEC offers a route to a range of new dynamics and phenomena, since the nonlinear effects of interatomic interactions introduce, on the mean-field level, the potential for true wave chaos [35–40,58,78–80]. For experimentally realistic interaction strengths and atom numbers, the key new dynamical features of the δ-kicked-rotor BEC, within a mean-field description, are the appearance of *nonlinear* quantum resonances (with no analog in the linear regime) and the appearance of sharp, asymmetric cutoffs in the resonance profiles as a function of driving period. Both these features were identified in Ref. [40] using the zeroth-order, GPE description.

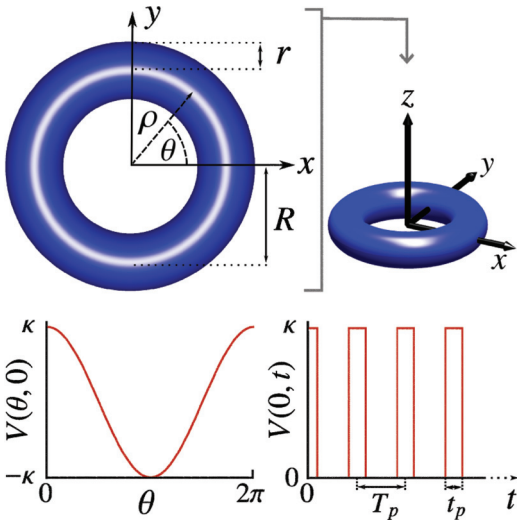

FIG. 2. (Color online) The δ-kicked-rotor-BEC system. A repulsively interacting atomic BEC consisting of N atoms is held in a quasi-1D, toroidally shaped trap, and driven by periodic kicks of short duration t_p, which can be modeled as δ-impulses, from a sinusoidal driving potential. The free parameters of the system are the dimensionless kick strength κ, kicking period T_p, and interaction strength g_T. See Sec. IV B for a full definition of these parameters.

However, the beyond-mean-field effects of condensate depletion and condensate-noncondensate interactions can be expected to play an increasing role for longer times in strongly nonequilibrium driven systems such as the δ-kicked-rotor BEC. As highlighted in the introduction to this manuscript, dealing with such dynamics within a mean-field treatment or truncated Wigner approximation can be challenging; these challenges appear to have precluded any treatments of the dynamics of the δ-kicked-rotor BEC using these methods.

Until recently, all explicitly beyond-mean-field studies of the δ-kicked-rotor BEC have been conducted using a first-order number-conserving description.[4] Unfortunately, the lack of a self-consistent back-action of the noncondensate on the condensate in the first-order number-conserving description led to unbounded growth of the noncondensate, and unphysical results at long times when close to resonance [36,37,39]. The same effect has also been observed in the similar δ-kicked-harmonic-oscillator BEC [35,58]. However, in contrast to the first-order description, the presence of a self-consistent back-action in the second-order number-conserving description makes it ideal for the description of such systems.

In Ref. [41] a restricted implementation of the numerical method of Sec. III, limited to the study of zero-temperature initial conditions (and the details of which were not reported in that work), was used to demonstrate explicitly that the self-consistent back-action of the noncondensate damps out initially rapid growth in the noncondensate, which would continue unbounded in the first-order description. We illustrate this further in Fig. 3, which shows the number evolution obtained using the first- and second-order number-conserving

[4]Note, however, that some aspects of beyond-mean-field dynamics were inferred from analysis of the GPE in Ref. [40].

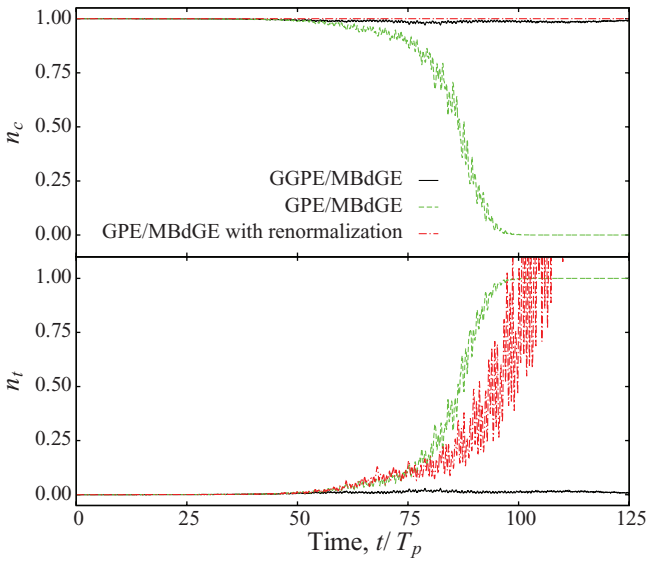

FIG. 3. (Color online) Zero-temperature evolution of the δ-kicked-rotor BEC close to a nonlinear resonance explored in Ref. [40] (dimensionless kick strength $\kappa = 0.5$, kick period $T_p = 6.12$, and interaction strength $g_T = 2.5 \times 10^{-4}$, and total atom number $N = 10^4$—see Sec. IV B). Beginning with a zero-temperature initial condition, three descriptions are used to determine the dynamics: the second-order number-conserving description [GGPE/MBdGE, Eqs. (14) and (19)], first-order number-conserving description [GPE/MBdGE, Eqs. (11) and (19)], and a first-order number-conserving description with *ad hoc* renormalization. In each case we show the evolution of the condensate fraction $n_c = N_c/N$ and the noncondensate fraction $n_t = N_t/N$. Note that, in the first-order description *without* renormalization, $n_c = 1$ for all times.

descriptions to evolve the dynamics of an initially zero-temperature δ-kicked-rotor BEC, for parameters close to a nonlinear resonance. In addition to the evolution of the first- and second-order descriptions, which were originally obtained in Ref. [41], we show the evolution of the same initial conditions under "renormalized" first-order equations of motion; these are identical to the first-order equations of motion, but with an added renormalization of the condensate, applied by explicitly calculating N_t and setting $N_c = N - N_t$ immediately after each time step. While it does prevent the occurrence of unphysical growth of the total particle number, this *ad hoc* renormalization procedure fails to damp out the rapid growth of the noncondensate in a similar way to the second-order description. This illustrates that the *self-consistent* nature of the back-action of the noncondensate in the second-order description is key to preventing unphysical growth of the noncondensate.

In the following sections we outline the exact procedure for applying the numerical method of Sec. III to the δ-kicked-rotor BEC. We then use the numerical model so developed to explore the dynamics of the δ-kicked-rotor BEC for finite-temperature initial conditions for the first time. While no particularly novel new physics is expected beyond that observed for zero-temperature initial conditions, this exploration nonetheless (a) demonstrates the efficacy of the method, (b) serves as a concrete example of how to apply the preceding formal developments to a specific problem, and (c) allows the first *quantitative* prediction of departures from the initially zero-temperature dynamics in the finite-temperature case. Since any future experiments on the system will necessarily operate at nonzero temperatures, such a quantitative prediction is particularly relevant in that regard.

B. Theoretical model and initial conditions

As shown in Fig. 2, we consider a system described by Hamiltonian [Eq. (1)] with a toroidal external potential $V_T(\rho,z) = m\omega^2[(\rho - R)^2 + z^2]/2$ [Fig. 2(a)]. Potentials similar to this have been experimentally realized in, e.g., Refs. [81,82]. We assume a sufficiently strong effective trap frequency ω that the harmonic oscillator length in this direction, $a_r = \sqrt{\hbar/m\omega} \ll R$. Under this assumption, a quasi-1D approximation is justified and yields the 1D model Hamiltonian [83]:

$$\hat{H} = \int d\theta \hat{\Psi}^\dagger(\theta)\left[-\frac{1}{2}\frac{\partial^2}{\partial\theta^2} + V(\theta,t) + \frac{g_T}{2}\hat{\Psi}^\dagger(\theta)\hat{\Psi}(\theta)\right]\hat{\Psi}(\theta), \tag{66}$$

where we have chosen to use length units of R, time units of $mR^2/\hbar$, and we have introduced the dimensionless interaction strength $g_T = 2a_s R/a_r^2$. Note that this choice of dimensionless units can be codified as $\hbar = m \;\; R = 1$. When working at finite temperature, we add $k_B = 1$ to this system of units. We restrict our analysis to the case where the system size, $2\pi R$, is much smaller than the phase coherence length $l_\phi = 2\pi R \exp(\sqrt{\pi N_c/2g_T})/\sqrt{4\pi g_T N_c}$; in this case the ground state of the system can contain a true homogeneous Bose-Einstein condensate [84]. We do not consider the alternative case of a quasicondensate ($l_\phi \lesssim 2\pi R$) [85,86].

As in previous studies of the δ-kicked-rotor BEC [36,37,39,40], we model the driving potential as a train of δ-kicks,

$$V(\theta,t) = \kappa\cos(\theta)\sum_{n=0}^{\infty}\delta(t - nT_p). \tag{67}$$

Here the dimensionless kicking period T_p is defined in terms of the real kick period $T_p^{(\mathrm{real})}$ as $T_p = \hbar T_p^{(\mathrm{real})}/mR^2$, and the dimensionless kick strength κ is dependent on the real strength of the driving potential, and its duration t_p. Such a driving potential may be approximated in experiment using, e.g., short pulses of off-resonant laser light [73–75]. Further details of the physical aspects of the system can be found in Refs. [40,41].

The equations of motion for the δ-kicked-rotor BEC are identical to those of Sec. II B with the replacement $\mathbf{r} \to \theta$. The dynamical and thermal equilibrium state of the system consists of a uniform condensate mode, $\psi(\theta) = \sqrt{N_c/2\pi}$, accompanied by a thermal population of Bogoliubov quasiparticle excitations. Both at $T = 0$ and for $T > 0$, the stationary initial Bogoliubov modes associated with the uniform condensate are given by Ref. [41]

$$\begin{pmatrix} u_k(\theta) \\ v_k(\theta) \end{pmatrix} = \frac{1}{2}\begin{pmatrix} C_k + C_k^{-1} \\ C_k - C_k^{-1} \end{pmatrix}\frac{e^{ik\theta}}{\sqrt{2\pi}}, \tag{68}$$

where

$$C_k = C_{-k} = \left(\frac{k^2}{k^2 + 4\lambda_0^{(2)}}\right)^{1/4}, \tag{69}$$

and, for the uniform initial condensate, $\lambda_0^{(2)} = g_T N_c/2\pi$. It is important to note that in this section we have replaced the completely generic quasiparticle index $k = 1,2,\ldots$ used in Sec. III with the quasiparticle momentum index $k = \ldots,-2,-1,1,2,\ldots$, as this considerably simplifies the notation. Consequently, in our numerical treatment we must also replace the generic quasiparticle cutoff momentum M with an explicit maximum quasiparticle momentum index $k_{\max}$. The expressions appearing in Sec. III can be reformulated in this new notation simply by making the replacements,

$$\sum_{k=1}^{M} \to \sum_{k=-k_{\max}}^{k_{\max}}{}', \tag{70}$$

$$M \to 2k_{\max}, \tag{71}$$

where $\sum'$ indicates a summation omitting the term $k = 0$ (which here corresponds to the condensate mode).

The energy of a quasiparticle of momentum k is given by

$$\epsilon_k = \sqrt{\frac{k^4}{4} + k^2\lambda_0^{(2)}}. \tag{72}$$

Hence, the noncondensate population can be determined from

$$\begin{aligned} N_t &= \int_0^{2\pi} d\theta \sum_{k=-k_{\max}}^{k_{\max}}{}' \left[N_k|u_k(\theta)|^2 + (N_k+1)|v_k(\theta)|^2\right] \\ &= \frac{1}{4}\sum_{k=-k_{\max}}^{k_{\max}}{}' \left[N_k\left(C_k + C_{-k}^{-1}\right)^2 + (N_k+1)\left(C_k - C_{-k}^{-1}\right)^2\right], \end{aligned} \tag{73}$$

where the populations N_k are obtained from the energies ϵ_k using the appropriate *thermal* Bose distribution [Eq. (37)]. Note that in our system of dimensionless variables, the dimensionless temperature T used to obtain populations corresponds to a real temperature through the relation $T_{\text{real}} = T\hbar^2/mR^2k_B$. Our procedure for finding a self-consistent initial condition thus represents an extension of the method used in Ref. [41], which allows us to simulate finite temperature dynamics.

To obtain a specific initial condition, we initially set $N_c = N$ and then: (a) calculate the coefficients C_k up to the momentum cutoff $k_{\max}$; (b) calculate N_t using Eq. (73); (c) renormalize the total number of atoms by reducing the condensate population to $N_c = N - N_t$. Steps (a)–(c) are then repeated until N_t converges to within 10^{-6} of its final value. We choose $k_{\max}$ sufficiently large that $N_{k_{\max}} < 10^{-2}$ (in addition to confirming that the subsequent dynamics have converged as a function of $k_{\max}$); this means that $k_{\max}$ increases substantially with temperature. However, for the temperatures we consider (up to $T = 300$) $k_{\max} = 64$ is sufficient, and the effect of the finite-size correction $\mu - \lambda_0^{(2)}$ is negligible. Finally, we numerically evaluate the GGPE eigenvalue $\bar{\lambda}_2^{(2)}$ for the obtained initial equilibrium condition. Evolution of the resulting initial condition is accomplished using the numerical method of Sec. III. We choose time steps which exactly divide the dimensionless kick period T_p, such that the effect of a kick can be accomplished via the instantaneous transformation,

$$\psi(\theta) \to e^{-i\kappa\cos\theta}\psi(\theta), \tag{74}$$

$$u_k(\theta) \to e^{-i\kappa\cos\theta}u_k(\theta), \tag{75}$$

$$v_k(\theta) \to e^{i\kappa\cos\theta}v_k(\theta), \tag{76}$$

which is applied at the exact instant of each kick. The resulting evolution is then checked for convergence in the number of grid points, quasiparticle momentum cutoff, and time step.

C. Finite-temperature dynamics

We now explore the dynamics of the δ-kicked rotor for a range of finite temperature equilibrium initial conditions. In addition to tracking the condensate fraction $n_c = N_c/N$ and noncondensate fraction $n_t = N_t/N$—variables which the number-conserving description gives immediate access to—we also introduce measures to track the presence of many-body, beyond-mean-field effects in the system. In Ref. [41], the quantity,

$$C = \iint d\theta d\theta' g_1(\theta,\theta')g_1(\theta',\theta), \tag{77}$$

which represents a spatial average of the first-order correlation function $g_1(\theta,\theta') = \langle\hat{\Psi}^\dagger(\theta')\hat{\Psi}(\theta)\rangle/N$, was introduced for this purpose. In terms of the single-particle density matrix $\rho(\theta,\theta')$, C can be defined as

$$C = \frac{\text{Tr}\{\rho(\theta,\theta')^2\}}{N^2}. \tag{78}$$

To an order consistent with the rest of the second-order number-conserving description, the single-particle density matrix $\rho(\theta,\theta')$ is given by

$$\begin{aligned} \rho(\theta,\theta') = \psi^*(\theta')\psi(\theta) &+ \sum_{k=-k_{\max}}^{k_{\max}}{}' \left[N_k u_k(\theta)u_k^*(\theta')\right] \\ &+ \sum_{k=-k_{\max}}^{k_{\max}}{}' \left[(N_k+1)v_k(\theta')v_k^*(\theta)\right]. \end{aligned} \tag{79}$$

The coherence measure C is thus analogous to the purity of a state in a single-particle system, defined by $\text{Tr}[\varrho^2]/(\text{Tr}[\varrho])^2$ (where ϱ is the full density matrix for the single-particle system). Using this measure an entirely condensed state (zero noncondensate fraction) is akin to a pure state of a single-particle system, and has $C = 1$. The presence of noncondensate—either in the form of the zero-temperature quantum depletion, or in the form of thermally excited quasiparticles—guarantees that $C < 1$. This is akin to a mixed state of a single-particle system. Physically, this can be interpreted as indicating the presence of high-order (many-body) correlations between the condensate and noncondensate; these are effectively "traced out" when one uses the number-conserving description to compute a single-particle density matrix, resulting in $\rho(\theta,\theta')$ appearing "mixed."

In this paper we introduce another measure which probes the underlying many-body correlations: the single-particle von Neumann entropy. This again is defined in terms of the single-particle density matrix, and is given by

$$S_{\text{sp}} = -\text{Tr}\left\{\frac{\rho}{N}\ln\left(\frac{\rho}{N}\right)\right\}. \tag{80}$$

In contrast to C, which is unity for a pure condensate, $S_{\rm sp} = 0$ for a pure condensate, and $S_{\rm sp} > 0$ otherwise. Much like C, however, $S_{\rm sp}$ gives an indication of the magnitude of the underlying many-body correlations and the degree of entanglement present in the system. It should be noted that as a direct measure of entanglement in a many-body system, $S_{\rm sp}$ is imperfect, as a proportion of its magnitude can be due to Bose symmetry rather than genuine entanglement (i.e., entanglement between particles not arising as a direct consequence of the Bose symmetry of the wave function [87–89]). However, its use as an *indicator* for such entanglement, as we use it here, is well established [87,90,91].

To explore the finite-temperature evolution of the δ-kicked-rotor BEC, we initially consider specific parameters ($T_p = 6.12$, $\kappa = 0.5$, $g_T = 2.5 \times 10^{-4}$, and $N = 10^4$) which are close to a nonlinear resonance; these parameters were previously subject to detailed analysis—using the GPE, the first-order number-conserving description, and the second-order number-conserving description—in Refs. [40] and [41]. Figure 5 shows the evolution of the δ-kicked-rotor BEC, for these parameters, resulting from three different equilibrium initial conditions with temperatures $T = 0$, $T = 100$, and $T = 300$. These dimensionless temperatures should be considered in the context of Fig. 4, which shows the condensate fraction in the equilibrium ground state of this system (calculated as described in Sec. IV B) within our second-order, number-conserving treatment. Within this treatment $T_c \approx 832$ is the effective critical temperature, above which it is no longer possible to converge a self-consistent equilibrium initial condition. Note, however, that we choose temperatures sufficiently low that $n_c > 0.8$ such that $\tilde{\Lambda}(\mathbf{r})$ remains a small parameter.

For each initial condition the condensate fraction n_c, noncondensate fraction n_t, coherence measure C, and single-particle von Neumann entropy $S_{\rm sp}$ are shown in Fig. 5. In each case, the coherence measure and single-particle von Neumann entropy follow the noncondensate fraction very closely. This indicates that depletion of the condensate is the dominant factor in creating many-body correlations and entanglement in this system.

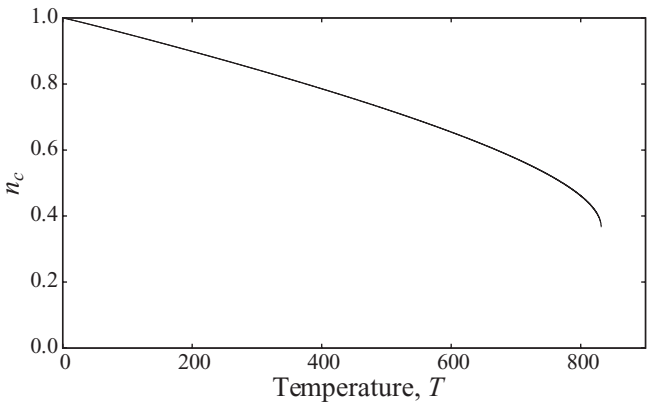

FIG. 4. Condensate fraction n_c in the equilibrium ground state of the δ-kicked-rotor BEC (parameters $g_T = 2.5 \times 10^{-4}$, $N = 10^4$) as a function of the dimensionless temperature T, calculated within the second-order number-conserving description. The point above which convergent solutions cannot be found gives an estimate of the condensation transition temperature $T_c \approx 832$ for this system. However, our second-order treatment is valid only for temperatures such that the small parameter $(1 - n_c)/n_c \ll 1$.

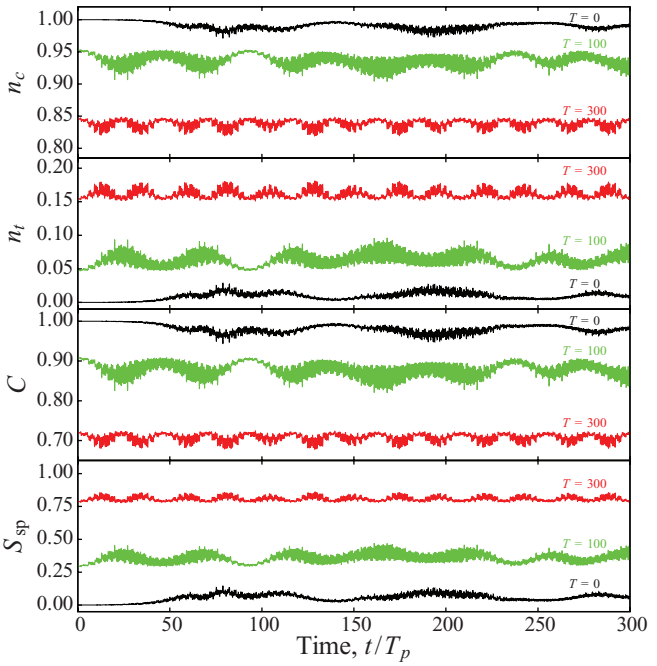

FIG. 5. (Color online) Finite-temperature evolution of the δ-kicked-rotor BEC close to a nonlinear resonance explored in [40] (parameters $g_T = 2.5 \times 10^{-4}$, $N = 10^4$, $T_p = 6.12$, $\kappa = 0.5$). Condensate and noncondensate fractions n_c and n_t, coherence measure C, and the single-particle von Neumann entropy $S_{\rm sp}$ are shown for initial temperatures $T = 0$, $T = 100$, and $T = 300$.

The most noticeable difference between the temperatures is in the initial noncondensate fraction (and consequently in the coherence and entropy, since these generally scale with n_t as explained above). This increase is to be expected, as the number of thermally excited quasiparticles increases as a function of temperature. The larger thermal population at higher temperatures also has the effect of significantly depleting the condensate, and hence reducing the effective nonlinearity, as given by the product $g_T N$. At zero temperature, the resonant kicking period is known to shift downwards as a function of the product $g_T N$, which represents the effective nonlinearity [40,41]. Hence, the presence of a thermal background, which effectively reduces $g_T N$, produces an upwards shift in the resonant kicking period. That this is the case is confirmed numerically in Fig. 6, in which we plot the overall response of the system—measured by the fractional population of all momentum modes higher than $k = 0$ among all atoms averaged over 100 kick periods (see [41])—as a function of kicking period T_p and temperature. Another interesting feature revealed by Fig. 6 is that the sharp cutoff at the upper limit of the shifted Talbot-time resonance (the large resonant area to the right of the graphs) first observed in Ref. [40] is qualitatively preserved at finite temperatures. This is interesting as these features are not present in the noninteracting limit $g_T N_c \to 0$, and one might therefore reasonably expect that the decrease in condensate population (and associated decrease in coherence) resulting from the increasing population of quasiparticles at finite temperature

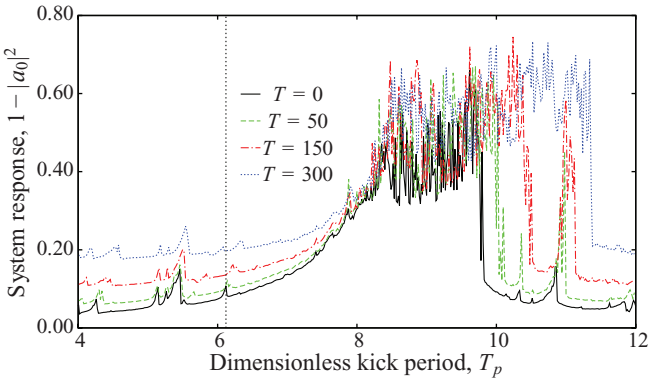

FIG. 6. (Color online) Finite-temperature shift of quantum resonances in the δ-kicked-rotor BEC. Parameters $g_T = 2.5 \times 10^{-4}$, $N = 2.5$, and $\kappa = 0.5$ have been chosen such that $T_p = 6.12$ (vertical dashed line) corresponds to the nonlinear resonance explored in [40,41] and Fig. 5. In particular, the finite-temperature shift in the location of this nonlinear resonance explains the nonresonant behavior seen at finite temperature in Fig. 5. Interestingly, the extremely sharp cutoffs observed in the GPE [40] and at zero temperature in the GGPE [41] are preserved at $T = 300$.

would gradually soften these features. However, we observe that the features remain sharp even with ∼20% depletion of the condensate.

While the dynamics of the system at the finite temperatures accessible with the second-order number-conserving description show no major qualitative differences to the initially zero-temperature case, the quantitative shifts in the positions of the resonances would be particularly relevant in the context of experiments aimed at studying nonlinear resonances in the δ-kicked-rotor BEC. For example, in an experiment with similar parameters to Ref. [82], the unit of temperature defined above takes a value ∼10 pK. Consequently, a future experiment with a temperature value in the range 1–10 nK would have dimensionless temperature $100 \lesssim T \lesssim 1000$ in the units used here. Our results show that the nonlinear resonances in such an experiment would thus be considerably shifted away from their zero-temperature values, and provide a quantitative prediction of this shift which could be experimentally tested. The preserved sharpness of the resonance cutoffs would help facilitate such a measurement.

V. CONCLUSIONS

We have described in detail a numerical method for evolving the integro-differential equations of motion of the second-order number-conserving description of Gardiner and Morgan [51]. This numerical method explicitly includes problematic nonlinear, nonlocal terms which are necessary in order to preserve orthogonality between condensate and noncondensate in this description. Our method provides a fully time-dependent, self-consistent treatment of number dynamics and condensate-noncondensate interactions in a finite-temperature BEC, and provides an excellent framework with which to study the nonequilibrium dynamics of driven BEC systems at low temperatures. We have used this numerical method to systematically study a prototypical example of such a system, the δ-kicked-rotor BEC, at finite temperature. While the qualitative features of the zero-temperature dynamics in this system are generally preserved at finite temperatures, our treatment nonetheless provides the first prediction of a quantitative shift in resonance frequencies at higher temperatures. This shift would be relevant for, and could feasibly be verified by, future experiments studying this system.

ACKNOWLEDGMENTS

We thank A. S. Bradley, S. Fishman, T. S. Monteiro, M. D. Lee, and H. Veksler for enlightening discussions, and acknowledge support from the United Kingdom Engineering and Physical Sciences Research Council (Grant No. EP/G056781/1), the Marsden Fund of New Zealand (Contract No. UOO162), and the Royal Society of New Zealand (Contract No. UOO004) (T.P.B.), Marie Curie Fellowship NUM2BEC (Grant No. 300285) (P.M.), and the Jack Dodd Centre and The Royal Society of London (Grant No. IE110202) (S.A.G.).

APPENDIX: MATRIX FORM OF THE EVOLUTION OPERATOR

1. Determination of eigenvalues

We wish to find a general analytic expression for the matrix form of $e^{-i\Gamma_N(\mathbf{r},t)\delta t/2\hbar}$ at a given position $\mathbf{r}$ and time t, where $\Gamma_N(\mathbf{r},t)$ is defined by

$$\Gamma_N(\mathbf{r},t) = \begin{pmatrix} H_N(\mathbf{r},t)+B(\mathbf{r},t) & (N_1+1)A_1(\mathbf{r},t) & (N_2+1)A_2(\mathbf{r},t) & \cdots & (N_M+1)A_M(\mathbf{r},t) & N_1A_1^*(\mathbf{r},t) & N_2A_2^*(\mathbf{r},t) & \cdots & N_MA_M^*(\mathbf{r},t) \\ A_1^*(\mathbf{r},t) & H_N(\mathbf{r},t) & 0 & \cdots & 0 & 0 & 0 & \cdots & 0 \\ A_2^*(\mathbf{r},t) & 0 & H_N(\mathbf{r},t) & \cdots & 0 & 0 & 0 & \cdots & 0 \\ \vdots & \vdots & \vdots & \ddots & \vdots & \vdots & \vdots & \cdots & \vdots \\ A_M^*(\mathbf{r},t) & 0 & 0 & \cdots & H_N(\mathbf{r},t) & 0 & 0 & \cdots & 0 \\ A_1(\mathbf{r},t) & 0 & 0 & \cdots & 0 & H_N(\mathbf{r},t) & 0 & \cdots & 0 \\ A_2(\mathbf{r},t) & 0 & 0 & \cdots & 0 & 0 & H_N(\mathbf{r},t) & \cdots & 0 \\ \vdots & \vdots & \vdots & \vdots & \vdots & \vdots & \vdots & \ddots & \vdots \\ A_M(\mathbf{r},t) & 0 & 0 & \cdots & 0 & 0 & 0 & \cdots & H_N(\mathbf{r},t) \end{pmatrix}, \tag{A1}$$

for

$$H_{\mathrm{N}}(\mathbf{r},t) = V(\mathbf{r},t) + U_0|\psi(\mathbf{r},t)|^2, \tag{A2}$$

and

$$B(\mathbf{r},t) = U_0\tilde{n}(\mathbf{r},\mathbf{r},t) - U_0\frac{|\psi(\mathbf{r},t)|^2}{N_c} - \lambda'. \tag{A3}$$

We will show that this exponentiation of $\Gamma_{\mathrm{N}}(\mathbf{r},t)$, at a given position and time, can be accomplished in a closed analytic form for arbitrary M. From this point forward, we adopt the clarifying convention of omitting the explicit position and time arguments $\mathbf{r}$ and t: All quantities appearing in our treatment should be interpreted as the complex, *scalar* values obtained by evaluating the corresponding $\mathbf{r}$- and t-dependent functions at a particular position and time.

We proceed by identifying all eigenvalues of the matrix Γ_{N} through the characteristic equation,

$$\det(\Gamma_{\mathrm{N}} - \xi I) = 0, \tag{A4}$$

where I is the $(2M+1)\times(2M+1)$ identity matrix. Expanding the determinant over minors of the first row yields

$$\det(\Gamma_{\mathrm{N}} - \xi I) = (H_{\mathrm{N}} + B - \xi)(H_{\mathrm{N}} - \xi)I - (N_1+1)A_1 \times \begin{vmatrix} A_1^* & 0 & \cdots & 0 & 0 & 0 & \cdots & 0 \\ A_2^* & H_{\mathrm{N}}-\xi & \cdots & 0 & 0 & 0 & \cdots & 0 \\ \vdots & \vdots & \ddots & \vdots & \vdots & \vdots & \cdots & \vdots \\ A_M^* & 0 & \cdots & H_{\mathrm{N}}-\xi & 0 & 0 & \cdots & 0 \\ A_1 & 0 & \cdots & 0 & H_{\mathrm{N}}-\xi & 0 & \cdots & 0 \\ A_2 & 0 & \cdots & 0 & 0 & H_{\mathrm{N}}-\xi & \cdots & 0 \\ \vdots & \vdots & \vdots & \vdots & \vdots & \vdots & \ddots & \vdots \\ A_M & 0 & \cdots & 0 & 0 & 0 & \cdots & H_{\mathrm{N}}-\xi \end{vmatrix}$$

$$+(N_2+1)A_2 \times \begin{vmatrix} A_1^* & H_{\mathrm{N}}-\xi & \cdots & 0 & 0 & 0 & \cdots & 0 \\ A_2^* & 0 & \cdots & 0 & 0 & 0 & \cdots & 0 \\ \vdots & \vdots & \ddots & \vdots & \vdots & \vdots & \cdots & \vdots \\ A_M^* & 0 & \cdots & H_{\mathrm{N}}-\xi & 0 & 0 & \cdots & 0 \\ A_1 & 0 & \cdots & 0 & H_{\mathrm{N}}-\xi & 0 & \cdots & 0 \\ A_2 & 0 & \cdots & 0 & 0 & H_{\mathrm{N}}-\xi & \cdots & 0 \\ \vdots & \vdots & \vdots & \vdots & \vdots & \vdots & \ddots & \vdots \\ A_M & 0 & \cdots & 0 & 0 & 0 & \cdots & H_{\mathrm{N}}-\xi \end{vmatrix} - \cdots, \tag{A5}$$

where the choice of $+$ and $-$ signs in later terms is dependent on the parity of M. The determinant of the first minor is trivially $(H_{\mathrm{N}}-\xi)^{2M}$, and the determinant of each subsequent minor is easily computed by further expanding in minors along the row containing no entry of the form $H_{\mathrm{N}}-\xi$. Carefully keeping track of signs, this yields

$$\det(\Gamma_{\mathrm{N}} - \xi I) = (H_{\mathrm{N}} + B - \xi)(H_{\mathrm{N}} - \xi)^{2M} + \sum_{k=1}^{M}(-1)^k(N_k+1)A_k(-1)^{k+1}A_k^*(H_{\mathrm{N}}-\xi)^{2M-1}$$
$$+ \sum_{k=1}^{M}(-1)^{M+k}N_kA_k^*(-1)^{M+k+1}A_k(H_{\mathrm{N}}-\xi)^{2M-1}, \tag{A6}$$

which simplifies to

$$\det(\Gamma_{\mathrm{N}} - \xi I) = [(H_{\mathrm{N}} + B - \xi)(H_{\mathrm{N}} - \xi) - \Sigma](H_{\mathrm{N}} - \xi)^{2M-1}, \tag{A7}$$

where

$$\Sigma = \sum_{k=1}^{M}(2N_k+1)|A_k|^2. \tag{A8}$$

Note that Eq. (A7) holds regardless of the parity of M. Consequently, $2M-1$ eigenvalues of Γ_{N} are degenerate, having value H_{N}. The remaining two eigenvalues ξ solve the quadratic equation,

$$[H_{\mathrm{N}} - \xi]^2 + B[H_{\mathrm{N}} - \xi] - \Sigma = 0, \tag{A9}$$

and hence are given by

$$\xi = H_{\mathrm{N}} + \frac{B}{2} \pm \sqrt{\left(\frac{B}{2}\right)^2 + \Sigma}. \tag{A10}$$

2. Determination of eigenvectors

A set of linearly independent eigenvectors ζ associated with the $2M-1$ degenerate eigenvalues $\xi = H_{\mathrm{N}}$ must be obtained

by solving the linear equations,

$$(\Gamma_{\mathrm{N}} - H_{\mathrm{N}} I)\,\zeta = 0. \tag{A11}$$

Such a set can be found by setting $\psi = 0$ in Eq. (A11), reducing the linear equations to

$$\sum_{k=1}^{M}[(N_k+1)A_k v_k^* + N_k A_k^* u_k] = 0. \tag{A12}$$

The required linearly independent solutions are given by

$$v_1^* = (N_k+1)A_k, \quad v_k^* = -\delta_{kj}(N_1+1)A_1, \quad u_k = 0, \tag{A13}$$

where $j \in \{2 \ldots M\}$, and

$$v_1^* = N_k A_k^*, \quad v_k^* = 0, \quad u_k = -\delta_{kj}(N_1+1)A_1, \tag{A14}$$

where $j \in \{1 \ldots M\}$.

For the remaining two eigenvalues one has to solve the linear equations,

$$\left\{\Gamma_{\mathrm{N}} - \left[H_{\mathrm{N}} + \left(\frac{B}{2} \pm \sqrt{\left(\frac{B}{2}\right)^2 + \Sigma}\right)\right] I\right\}\zeta = 0, \tag{A15}$$

which can be expressed as the system,

$$A_k^*\psi - \left(\frac{B}{2} \pm \sqrt{\left(\frac{B}{2}\right)^2 + \Sigma}\right) v_k^* = 0, \tag{A16}$$

$$A_k\psi - \left(\frac{B}{2} \pm \sqrt{\left(\frac{B}{2}\right)^2 + \Sigma}\right) u_k = 0, \tag{A17}$$

$$\left(\frac{B}{2} \mp \sqrt{\left(\frac{B}{2}\right)^2 + \Sigma}\right)\psi + \sum_{k=1}^{M}(N_k+1)A_k v_k^* + \sum_{k=1}^{M} N_k A_k^* u_k = 0. \tag{A18}$$

Rearranging the first two equations to obtain

$$v_k^* = \frac{A_k^*}{\frac{B}{2} \pm \sqrt{\left(\frac{B}{2}\right)^2 + \Sigma}}\psi, \tag{A19}$$

$$u_k = \frac{A_k}{\frac{B}{2} \pm \sqrt{\left(\frac{B}{2}\right)^2 + \Sigma}}\psi, \tag{A20}$$

provides a solution for arbitrary ψ, since substituting the above expressions into the third equation yields

$$\left[\left(\frac{B}{2} \mp \sqrt{\left(\frac{B}{2}\right)^2 + \Sigma}\right)\left(\frac{B}{2} \pm \sqrt{\left(\frac{B}{2}\right)^2 + \Sigma}\right) + \Sigma\right]\psi = 0, \tag{A21}$$

and hence

$$\left\{\left(\frac{B}{2}\right)^2 - \left[\left(\frac{B}{2}\right)^2 + \Sigma\right] + \Sigma\right\}\psi = 0, \tag{A22}$$

which is indeed satisfied for all ψ.

In the absence of any overriding scheme for normalizing the eigenvectors, a practically useful approach is to eliminate denominators in the transformation matrix P which has the eigenvectors as its columns. Choosing such a normalization, P is given by

$$P = \begin{pmatrix}
B_+ & B_- & 0 & \cdots & 0 & 0 & 0 & \cdots & 0 \\
A_1^* & A_1^* & (N_2+1)A_2 & \cdots & (N_M+1)A_M & N_1 A_1^* & N_2 A_2^* & \cdots & N_M A_M^* \\
A_2^* & A_2^* & -(N_1+1)A_1 & \cdots & 0 & 0 & 0 & \cdots & 0 \\
\vdots & \vdots & \vdots & \ddots & \vdots & \vdots & \vdots & \cdots & \vdots \\
A_M^* & A_M^* & 0 & \cdots & -(N_1+1)A_1 & 0 & 0 & \cdots & 0 \\
A_1 & A_1 & 0 & \cdots & 0 & -(N_1+1)A_1 & 0 & \cdots & 0 \\
A_2 & A_2 & 0 & \cdots & 0 & 0 & -(N_1+1)A_1 & \cdots & 0 \\
\vdots & \vdots & \vdots & \vdots & \vdots & \vdots & \vdots & \ddots & \vdots \\
A_M & A_M & 0 & \cdots & 0 & 0 & 0 & \cdots & -(N_1+1)A_1
\end{pmatrix}, \tag{A23}$$

where

$$B_\pm = \frac{B}{2} \pm \sqrt{\left(\frac{B}{2}\right)^2 + \Sigma}. \tag{A24}$$

3. Matrix exponentiation

In order to exponentiate the matrix Γ_{N}, one also requires the inverse P^{-1} of the transformation matrix P. Note that, since Γ_{N} is not Hermitian, P is not unitary, and $P^{-1} \neq P^\dagger$. However, P can nonetheless be inverted, for nonzero A_k, by a lengthy series

of elementary row operations. This yields

$$P^{-1}=\frac{1}{\Sigma}\begin{pmatrix}
\frac{\Sigma}{B_+-B_-} & C_-(N_1+1)A_1 & C_-(N_2+1)A_2 & \cdots & C_-(N_M+1)A_M & C_-N_1A_1^* & C_-N_2A_2^* & \cdots & C_-N_MA_M^* \\
\frac{-\Sigma}{B_+-B_-} & C_+(N_1+1)A_1 & C_+(N_2+1)A_2 & \cdots & C_+(N_M+1)A_M & C_+N_1A_1^* & C_+N_2A_2^* & \cdots & C_+N_MA_M^* \\
0 & \frac{A_2^*(N_1+1)A_1}{(N_1+1)A_1} & \frac{A_2^*(N_2+1)A_2-\Sigma}{(N_1+1)A_1} & \cdots & \frac{A_2^*(N_M+1)A_M}{(N_1+1)A_1} & \frac{A_2^*N_1A_1^*}{(N_1+1)A_1} & \frac{A_2^*N_2A_2^*}{(N_1+1)A_1} & \cdots & \frac{A_2^*N_MA_M^*}{(N_1+1)A_1} \\
\vdots & \vdots & \vdots & \ddots & \vdots & \vdots & \vdots & \cdots & \vdots \\
0 & \frac{A_M^*(N_1+1)A_1}{(N_1+1)A_1} & \frac{A_M^*(N_2+1)A_2}{(N_1+1)A_1} & \cdots & \frac{A_M^*(N_M+1)A_M-\Sigma}{(N_1+1)A_1} & \frac{A_M^*N_1A_1^*}{(N_1+1)A_1} & \frac{A_M^*N_2A_2^*}{(N_1+1)A_1} & \cdots & \frac{A_M^*N_MA_M^*}{(N_1+1)A_1} \\
0 & \frac{A_1(N_1+1)A_1}{(N_1+1)A_1} & \frac{A_1(N_2+1)A_2}{(N_1+1)A_1} & \cdots & \frac{A_1(N_M+1)A_M}{(N_1+1)A_1} & \frac{A_1N_1A_1^*-\Sigma}{(N_1+1)A_1} & \frac{A_1N_2A_2^*}{(N_1+1)A_1} & \cdots & \frac{A_1N_MA_M^*}{(N_1+1)A_1} \\
0 & \frac{A_2(N_1+1)A_1}{(N_1+1)A_1} & \frac{A_2(N_2+1)A_2}{(N_1+1)A_1} & \cdots & \frac{A_2(N_M+1)A_M}{(N_1+1)A_1} & \frac{A_2N_1A_1^*}{(N_1+1)A_1} & \frac{A_2N_2A_2^*-\Sigma}{(N_1+1)A_1} & \cdots & \frac{A_2N_MA_M^*}{(N_1+1)A_1} \\
\vdots & \vdots & \vdots & \vdots & \vdots & \vdots & \vdots & \ddots & \vdots \\
0 & \frac{A_M(N_1+1)A_1}{(N_1+1)A_1} & \frac{A_M(N_2+1)A_2}{(N_1+1)A_1} & \cdots & \frac{A_M(N_M+1)A_M}{(N_1+1)A_1} & \frac{A_MN_1A_1^*}{(N_1+1)A_1} & \frac{A_MN_2A_2^*}{(N_1+1)A_1} & \cdots & \frac{A_MN_MA_M^*-\Sigma}{(N_1+1)A_1}
\end{pmatrix}, \tag{A25}$$

where

$$C_\pm=\frac{1}{2}\pm\frac{B}{4\sqrt{\left(\frac{B}{2}\right)^2+\Sigma}}. \tag{A26}$$

Now we have $\Gamma_{\rm N}=PDP^{-1}$, where D is the diagonal matrix of the eigenvalues of $\Gamma_{\rm N}$. Consequently, we can compute the matrix exponential,

$$e^{-i\Gamma_{\rm N}\delta t/2\hbar}=Pe^{-iD\delta t/2\hbar}P^{-1}, \tag{A27}$$

using the results we have obtained up to this point. Using the identity,

$$C_-B_+=-C_+B_-=\frac{\Sigma}{2\sqrt{\left(\frac{B}{2}\right)^2+\Sigma}}, \tag{A28}$$

and with careful treatment of all summations, one obtains

$$\begin{aligned}
&e^{-i\Gamma_{\rm N}\delta t/2\hbar}\\
&=\begin{pmatrix}
T_{\rm cos}-\frac{BT_{\rm sin}}{2} & -(N_1+1)A_1T_{\rm sin} & -(N_2+1)A_2T_{\rm sin} & \cdots & -(N_M+1)A_MT_{\rm sin} & -N_1A_1^*T_{\rm sin} & -N_2A_2^*T_{\rm sin} & \cdots & -N_MA_M^*T_{\rm sin} \\
-A_1^*T_{\rm sin} & A_1^*(N_1+1)A_1T_{\rm mix} & A_1^*(N_2+1)A_2T_{\rm mix} & \cdots & A_1^*(N_M+1)A_MT_{\rm mix} & A_1^*N_1A_1^*T_{\rm mix} & A_1^*N_2A_2^*T_{\rm mix} & \cdots & A_1^*N_MA_M^*T_{\rm mix} \\
-A_2^*T_{\rm sin} & A_2^*(N_1+1)A_1T_{\rm mix} & A_2^*(N_2+1)A_2T_{\rm mix} & \cdots & A_2^*(N_M+1)A_MT_{\rm mix} & A_2^*N_1A_1^*T_{\rm mix} & A_2^*N_2A_2^*T_{\rm mix} & \cdots & A_2^*N_MA_M^*T_{\rm mix} \\
\vdots & \vdots & \vdots & \ddots & \vdots & \vdots & \vdots & \cdots & \vdots \\
-A_M^*T_{\rm sin} & A_M^*(N_1+1)A_1T_{\rm mix} & A_M^*(N_2+1)A_2T_{\rm mix} & \cdots & A_M^*(N_M+1)A_MT_{\rm mix} & A_M^*N_1A_1^*T_{\rm mix} & A_M^*N_2A_2^*T_{\rm mix} & \cdots & A_M^*N_MA_M^*T_{\rm mix} \\
-A_1T_{\rm sin} & A_1(N_1+1)A_1T_{\rm mix} & A_1(N_2+1)A_2T_{\rm mix} & \cdots & A_1(N_M+1)A_MT_{\rm mix} & A_1N_1A_1^*T_{\rm mix} & A_1N_2A_2^*T_{\rm mix} & \cdots & A_1N_MA_M^*T_{\rm mix} \\
-A_2T_{\rm sin} & A_2(N_1+1)A_1T_{\rm mix} & A_2(N_2+1)A_2T_{\rm mix} & \cdots & A_2(N_M+1)A_MT_{\rm mix} & A_2N_1A_1^*T_{\rm mix} & A_2N_2A_2^*T_{\rm mix} & \cdots & A_2N_MA_M^*T_{\rm mix} \\
\vdots & \vdots & \vdots & \vdots & \vdots & \vdots & \vdots & \ddots & \vdots \\
-A_MT_{\rm sin} & A_M(N_1+1)A_1T_{\rm mix} & A_M(N_2+1)A_2T_{\rm mix} & \cdots & A_M(N_M+1)A_MT_{\rm mix} & A_MN_1A_1^*T_{\rm mix} & A_MN_2A_2^*T_{\rm mix} & \cdots & A_MN_MA_M^*T_{\rm mix}
\end{pmatrix}\\
&\quad+\begin{pmatrix}
0 & 0 & 0 & \cdots & 0 \\
0 & T_{\rm exp} & 0 & \cdots & 0 \\
0 & 0 & T_{\rm exp} & \cdots & 0 \\
\vdots & \vdots & \vdots & \ddots & \vdots \\
0 & 0 & 0 & \cdots & T_{\rm exp}
\end{pmatrix},
\end{aligned} \tag{A29}$$

where

$$T_{\rm exp}=\exp\left(-iH_{\rm N}\frac{\delta t}{2\hbar}\right), \tag{A30}$$

$$T_{\cos} = \cos\left(\left[\left(\frac{B}{2}\right)^2 + \Sigma\right]^{\frac{1}{2}} \frac{\delta t}{2\hbar}\right) \exp\left(-i\left[H_{\rm N} + \frac{B}{2}\right]\frac{\delta t}{2\hbar}\right), \tag{A31}$$

$$T_{\sin} = i\sin\left(\left[\left(\frac{B}{2}\right)^2 + \Sigma\right]^{\frac{1}{2}} \frac{\delta t}{2\hbar}\right) \exp\left(-i\left[H_{\rm N} + \frac{B}{2}\right]\frac{\delta t}{2\hbar}\right)\left[\left(\frac{B}{2}\right)^2 + \Sigma\right]^{-\frac{1}{2}}, \tag{A32}$$

$$T_{\rm mix} = \frac{T_{\cos} + \frac{1}{2}T_{\sin}B - T_{\exp}}{\Sigma}. \tag{A33}$$

Thus, the action of the operator $e^{-i\Gamma_{\rm N}\delta t/2\hbar}$ can be succinctly expressed as $2M+1$ coupled equations:

$$\psi(\mathbf{r},t+\delta t/2) = \left(T_{\cos}(\mathbf{r},t) - \tfrac{1}{2}T_{\sin}(\mathbf{r},t)B(\mathbf{r},t)\right)\psi(\mathbf{r},t) - T_{\sin}(\mathbf{r},t)\Xi(\mathbf{r},t), \tag{A34}$$

$$v_k^*(\mathbf{r},t+\delta t/2) = -A_k^*(\mathbf{r},t)T_{\sin}(\mathbf{r},t)\psi(\mathbf{r},t) + T_{\exp}(\mathbf{r},t)v_k^*(\mathbf{r},t) + A_k^*(\mathbf{r},t)T_{\rm mix}(\mathbf{r},t)\Xi(\mathbf{r},t), \tag{A35}$$

$$u_k(\mathbf{r},t+\delta t/2) = -A_k(\mathbf{r},t)T_{\sin}(\mathbf{r},t)\psi(\mathbf{r},t) + T_{\exp}(\mathbf{r},t)u_k(\mathbf{r},t) + A_k(\mathbf{r},t)T_{\rm mix}(\mathbf{r},t)\Xi(\mathbf{r},t), \tag{A36}$$

where

$$\Xi(\mathbf{r},t) = \sum_{l=1}^{M}(N_l+1)A_l(\mathbf{r},t)v_l^*(\mathbf{r},t) + N_l A_l^*(\mathbf{r},t)u_l(\mathbf{r},t), \tag{A37}$$

and we have explicitly indicated all space and time dependence for clarity. Equations (A34)–(A37) appear in the main text as Eqs. (57)–(60), and constitute the central result of this Appendix.

[1] S. A. Gardiner, J. Mod. Opt. **49**, 1971 (2002).
[2] N. P. Proukakis and B. Jackson, J. Phys. B **41**, 203002 (2008).
[3] T. Gasenzer and J. M. Pawlowski, Phys. Lett. B **670**, 135 (2008).
[4] D. A. W. Hutchinson, E. Zaremba, and A. Griffin, Phys. Rev. Lett. **78**, 1842 (1997).
[5] R. J. Dodd, M. Edwards, C. W. Clark, and K. Burnett, Phys. Rev. A **57**, R32 (1998).
[6] J. Reidl, A. Csordás, R. Graham, and P. Szépfalusy, Phys. Rev. A **59**, 3816 (1999).
[7] S. Giorgini, Phys. Rev. A **57**, 2949 (1998).
[8] E. Zaremba, T. Nikuni, and A. Griffin, J. Low Temp. Phys. **116**, 277 (1999).
[9] A. Griffin, T. Nikuni, and E. Zaremba, *Bose-Condensed Gases at Finite Temperatures* (Cambridge University Press, Cambridge, 2009).
[10] B. Jackson and E. Zaremba, Phys. Rev. Lett. **87**, 100404 (2001).
[11] B. Jackson and E. Zaremba, Phys. Rev. Lett. **89**, 150402 (2002).
[12] J. E. Williams, E. Zaremba, B. Jackson, T. Nikuni, and A. Griffin, Phys. Rev. Lett. **88**, 070401 (2002).
[13] B. Jackson, N. P. Proukakis, C. F. Barenghi, and E. Zaremba, Phys. Rev. A **79**, 053615 (2009).
[14] B. Jackson, N. P. Proukakis, and C. F. Barenghi, Phys. Rev. A **75**, 051601 (2007).
[15] P. B. Blakie, A. S. Bradley, M. J. Davis, R. J. Ballagh, and C. W. Gardiner, Adv. Phys. **57**, 363 (2008).
[16] M. J. Davis, S. A. Morgan, and K. Burnett, Phys. Rev. Lett. **87**, 160402 (2001).
[17] M. J. Davis and P. B. Blakie, Phys. Rev. Lett. **96**, 060404 (2006).
[18] T. P. Simula and P. B. Blakie, Phys. Rev. Lett. **96**, 020404 (2006).
[19] C. W. Gardiner, J. R. Anglin, and T. I. A. Fudge, J. Phys. B **35**, 1555 (2002).
[20] A. S. Bradley, C. W. Gardiner, and M. J. Davis, Phys. Rev. A **77**, 033616 (2008).
[21] H. T. C. Stoof, Phys. Rev. Lett. **78**, 768 (1997).
[22] S. P. Cockburn and N. P. Proukakis, Laser Physics **19**, 558 (2009).
[23] S. P. Cockburn, H. E. Nistazakis, T. P. Horikis, P. G. Kevrekidis, N. P. Proukakis, and D. J. Frantzeskakis, Phys. Rev. Lett. **104**, 174101 (2010).
[24] C. N. Weiler, T. W. Neely, D. R. Scherer, A. S. Bradley, M. J. Davis, and B. P. Anderson, Nature (London) **455**, 948 (2008).
[25] T. W. Neely, E. C. Samson, A. S. Bradley, M. J. Davis, and B. P. Anderson, Phys. Rev. Lett. **104**, 160401 (2010).
[26] O. Fialko, A. S. Bradley, and J. Brand, Phys. Rev. Lett. **108**, 015301 (2012).
[27] C. Lobo, A. Sinatra, and Y. Castin, Phys. Rev. Lett. **92**, 020403 (2004).
[28] A. A. Norrie, R. J. Ballagh, and C. W. Gardiner, Phys. Rev. A **73**, 043617 (2006).
[29] R. G. Scott, T. E. Judd, and T. M. Fromhold, Phys. Rev. Lett. **100**, 100402 (2008).
[30] A. D. Martin and J. Ruostekoski, New J. Phys. **14**, 043040 (2012).
[31] Z.-Y. Ma, M. B. d'Arcy, and S. A. Gardiner, Phys. Rev. Lett. **93**, 164101 (2004).
[32] S. Schlunk, M. B. d'Arcy, S. A. Gardiner, and G. S. Summy, Phys. Rev. Lett. **90**, 124102 (2003).
[33] T. P. Billam and S. A. Gardiner, Phys. Rev. A **80**, 023414 (2009).
[34] S. A. Gardiner, J. I. Cirac, and P. Zoller, Phys. Rev. Lett. **79**, 4790 (1997).
[35] S. A. Gardiner, D. Jaksch, R. Dum, J. I. Cirac, and P. Zoller, Phys. Rev. A **62**, 023612 (2000).
[36] C. Zhang, J. Liu, M. G. Raizen, and Q. Niu, Phys. Rev. Lett. **92**, 054101 (2004).

[37] J. Liu, C. Zhang, M. G. Raizen, and Q. Niu, Phys. Rev. A **73**, 013601 (2006).
[38] D. L. Shepelyansky, Phys. Rev. Lett. **70**, 1787 (1993).
[39] J. Reslen, C. E. Creffield, and T. S. Monteiro, Phys. Rev. A **77**, 043621 (2008).
[40] T. S. Monteiro, A. Rançon, and J. Ruostekoski, Phys. Rev. Lett. **102**, 014102 (2009).
[41] T. P. Billam and S. A. Gardiner, New J. Phys. **14**, 013038 (2012).
[42] S. Schlunk, M. B. d'Arcy, S. A. Gardiner, D. Cassettari, R. M. Godun, and G. S. Summy, Phys. Rev. Lett. **90**, 054101 (2003).
[43] C. Weiss and N. Teichmann, Phys. Rev. Lett. **100**, 140408 (2008).
[44] A. Polkovnikov, K. Sengupta, A. Silva, and M. Vengalattore, Rev. Mod. Phys. **83**, 863 (2011).
[45] V. Yukalov, Laser Phys. Lett. **8**, 485 (2011).
[46] V. A. Yurovsky and M. Olshanii, Phys. Rev. Lett. **106**, 025303 (2011).
[47] A. D. Martin and J. Ruostekoski, in *Quantum Gases: Finite Temperature and Non-equilibrium Dynamics*, edited by N. P. Proukakis, S. A. Gardiner, M. Davis, and M. Szymanska (Imperial College Press, London, 2013), Chap. 13.
[48] T. M. Wright, N. P. Proukakis, and M. J. Davis, Phys. Rev. A **84**, 023608 (2011).
[49] A. Sinatra, C. Lobo, and Y. Castin, J. Phys. B **35**, 3599 (2002).
[50] A. J. Allen, C. F. Barenghi, N. P. Proukakis, and E. Zaremba, in *Quantum Gases: Finite Temperature and Non-equilibrium Dynamics*, edited by N. P. Proukakis, S. A. Gardiner, M. Davis, and M. Szymanska (Imperial College Press, London, 2013), Chap. 5.
[51] S. A. Gardiner and S. A. Morgan, Phys. Rev. A **75**, 043621 (2007).
[52] Y. Castin and R. Dum, Phys. Rev. A **57**, 3008 (1998).
[53] C. W. Gardiner, Phys. Rev. A **56**, 1414 (1997).
[54] M. Girardeau and R. Arnowitt, Phys. Rev. **113**, 755 (1959).
[55] M. D. Girardeau, Phys. Rev. A **58**, 775 (1998).
[56] S. A. Morgan, J. Phys. B **33**, 3847 (2000).
[57] O. Penrose and L. Onsager, Phys. Rev. **104**, 576 (1956).
[58] L. Rebuzzini, R. Artuso, S. Fishman, and I. Guarneri, Phys. Rev. A **76**, 031603 (2007).
[59] S. A. Morgan, M. Rusch, D. A. W. Hutchinson, and K. Burnett, Phys. Rev. Lett. **91**, 250403 (2003).
[60] S. A. Morgan, Phys. Rev. A **69**, 023609 (2004).
[61] S. A. Morgan, Phys. Rev. A **72**, 043609 (2005).
[62] D. S. Jin, J. R. Ensher, M. R. Matthews, C. E. Wieman, and E. A. Cornell, Phys. Rev. Lett. **77**, 420 (1996).
[63] D. S. Jin, M. R. Matthews, J. R. Ensher, C. E. Wieman, and E. A. Cornell, Phys. Rev. Lett. **78**, 764 (1997).
[64] M.-O. Mewes, M. R. Andrews, N. J. van Druten, D. M. Kurn, D. S. Durfee, C. G. Townsend, and W. Ketterle, Phys. Rev. Lett. **77**, 988 (1996).
[65] D. M. Stamper-Kurn, H.-J. Miesner, S. Inouye, M. R. Andrews, and W. Ketterle, Phys. Rev. Lett. **81**, 500 (1998).
[66] S. A. Gardiner and T. P. Billam, in *Quantum Gases: Finite Temperature and Non-equilibrium Dynamics*, edited by N. P. Proukakis, S. A. Gardiner, M. Davis, and M. Szymanska (Imperial College Press, London, 2013), Chap. 8.
[67] T. Köhler and K. Burnett, Phys. Rev. A **65**, 033601 (2002).
[68] F. Mandl, *Statistical Physics* (Wiley, New York, 1988).
[69] J. Javanainen and J. Ruostekoski, J. Phys. A **39**, L179 (2006).
[70] G. Golub and C. Van Loan, *Matrix Computations* (Johns Hopkins University Press, Baltimore, 1996).
[71] G. Casati, B. V. Chirikov, F. M. Izrailev, and J. Ford, *Stochastic Behavior in Classical and Quantum Hamiltonian Systems* (Springer, Berlin, 1979) .
[72] F. M. Izrailev and D. L. Shepelyanskii, Theor. Math. Phys. **43**, 553 (1980).
[73] M. Saunders, P. L. Halkyard, K. J. Challis, and S. A. Gardiner, Phys. Rev. A **76**, 043415 (2007).
[74] C. Ryu, M. F. Andersen, A. Vaziri, M. B. d'Arcy, J. M. Grossman, K. Helmerson, and W. D. Phillips, Phys. Rev. Lett. **96**, 160403 (2006).
[75] F. L. Moore, J. C. Robinson, C. F. Bharucha, B. Sundaram, and M. G. Raizen, Phys. Rev. Lett. **75**, 4598 (1995).
[76] M. K. Oberthaler, R. M. Godun, M. B. d'Arcy, G. S. Summy, and K. Burnett, Phys. Rev. Lett. **83**, 4447 (1999).
[77] G. J. Duffy, A. S. Mellish, K. J. Challis, and A. C. Wilson, Phys. Rev. A **70**, 041602 (2004).
[78] S. Wimberger, R. Mannella, O. Morsch, and E. Arimondo, Phys. Rev. Lett. **94**, 130404 (2005).
[79] L. Rebuzzini, S. Wimberger, and R. Artuso, Phys. Rev. E **71**, 036220 (2005).
[80] B. Mieck and R. Graham, J. Phys. A **38**, L139 (2005).
[81] S. Franke-Arnold, J. Leach, M. J. Padgett, V. E. Lembessis, D. Ellinas, A. J. Wright, J. M. Girkin, P. Öhberg, and A. S. Arnold, Opt. Express **15**, 8619 (2007).
[82] A. Ramanathan, K. C. Wright, S. R. Muniz, M. Zelan, W. T. Hill, C. J. Lobb, K. Helmerson, W. D. Phillips, and G. K. Campbell, Phys. Rev. Lett. **106**, 130401 (2011).
[83] P. L. Halkyard, M. P. A. Jones, and S. A. Gardiner, Phys. Rev. A **81**, 061602 (2010).
[84] A. G. Sykes, M. J. Davis, and D. C. Roberts, Phys. Rev. Lett. **103**, 085302 (2009).
[85] Yu. Kagan, B. Svistunov, and G. Shlyapnikov, Sov. Phys. JETP **66**, 314 (1987) [Zh. Eksp. Teor. Fiz. **93**, 552 (1987)].
[86] C. Mora and Y. Castin, Phys. Rev. A **67**, 053615 (2003).
[87] L. Amico, R. Fazio, A. Osterloh, and V. Vedral, Rev. Mod. Phys. **80**, 517 (2008).
[88] G. Ghirardi and L. Marinatto, Opt. Spectrosc. **99**, 386 (2005).
[89] V. Vedral, Central Eur. J. Phys. **1**, 289 (2003).
[90] A. Vardi and J. R. Anglin, Phys. Rev. Lett. **86**, 568 (2001).
[91] T. Sowiński, M. Brewczyk, M. Gajda, and K. Rzążewski, Phys. Rev. A **82**, 053631 (2010).